

INNOVATION IN AUGMENTING HIP AND
ANKLE PERFORMANCE DURING WALKING

By Leah K. Liebelt

A Thesis

Submitted in Partial Fulfillment
of the Requirements for the Degree of
Master of Science in
Mechanical Engineering

Northern Arizona University

April 2021

Approved:

Zachary F. Lerner, Ph.D., Chair

Michael Shafer, Ph.D.

Sarah Oman, Ph.D.

ABSTRACT

INNOVATION IN AUGMENTING HIP AND ANKLE PERFORMANCE DURING WALKING

LEAH K LIEBELT

This thesis considers two topics: hip assistance using a powered exoskeleton, and ankle assistance using a passive ankle-foot orthosis during walking. Part A introduces a lightweight bilateral hip exoskeleton used for improving gait function. Part B introduces an adjustable ankle foot orthosis to assist with ankle correction.

Exoskeletons are wearable robotic devices that can assist with a variety of tasks, such as load carrying, walking, or rehabilitation. In Part A, I introduce an ultra-lightweight hip exoskeleton aimed at assisting individuals with Cerebral Palsy and other gait impairments during rehabilitation or gait training exercises. This thesis presents the mechanical design and validation of the exoskeleton. The final mechanical design of the hip exoskeleton was derived through several prototypes, and verified for specific engineering requirements: weight, torque application, range of motion, and user comfort. A summary of the hip exoskeleton control system is briefly discussed.

Ankle-foot orthoses (AFOs) are devices commonly utilized for gait correction. AFOs are boot-like structures that encase the foot and lower leg to provide extra support and stability to the user during everyday tasks. Current market AFOs are extremely rigid, making walking difficult for individuals due to reduced ankle movement. Part B of this thesis introduces an adjustable AFO to help individuals increase their ankle motion while also aiding ankle power during stance and swing phases of the gait cycle. The final design of the AFO was derived through a single prototype, and validated for specific engineering requirements: weight, spring stiffness, modification ability, range of motion, and comfort.

Acknowledgements

First and foremost, I would like to thank my advisor Dr. Zach Lerner for his guidance and support over the last three years. His mentorship and passion to work on devices that improve lives helped shape me into the engineer I am today.

I would also like to thank my advisory committee, Dr. Michael Shafer and Dr. Sarah Oman, for their feedback and volunteered time to support my thesis defense.

Finally, I would like to thank the members of the NAU Biomechatronics Lab for their never-ending support throughout my project. I am continually humbled by the work they do and will forever be thankful I was a part of it.

Table of Contents

ABSTRACT.....	ii
Acknowledgements	iii
Table of contents	iv
List of Tables	vi
List of Figures	vii
1 Introduction	1
1.1 Movement Impairments	1
1.2 Treatments.....	1
Part A: The Design and Validation of a Powered Hip Exoskeleton	
2 Background	5
2.1 Hip Kinematics	5
2.2 Kinematics for Impaired Individuals	7
2.3 Relevance to Field.....	8
2.4 Exoskeletons	9
3 Literature Review	11
3.1 Rigid Exoskeletons	11
3.1.1 Samsung Institute of Technology GEMS Device	11
3.1.2 HONDA Device.....	12
3.1.3 BLEEX.....	15
3.1.4 PH-EXOS.....	16
3.1.5 Lightweight Active Pelvis Orthosis (APO).....	18
3.1.6 University of Utah’s Unilateral Hip Exoskeleton	19
3.2 Soft Exoskeletons.....	21
3.2.1 Soft Exosuit.....	21
3.2.2 Ankle-Hip Soft Exosuit.....	22
4 Design Criteria	24
4.1 Bilateral-dual assistance.....	24
4.2 Weight.....	24
4.3 Range of Motion	24
4.4 User Fit and Comfort	25
4.5 Lateral Protrusion.....	25
4.6 Torque Application	25
5 Design Concepts	27
5.1 Mechanical Design.....	27
5.1.1 Prototype A	27
5.1.2 Prototype B	29
5.1.3 Final Design.....	32
5.2 Control System.....	34
5.2.1 Bang-Bang	34
5.2.2 Proportional.....	35
6 Design Validation	36
6.1 Weight.....	36
6.2 Torque Tracking.....	37
6.3 Maximum Torque	38
6.4 User Fit.....	38
6.5 Comfort	39
6.6 Protruding Distance	39
6.7 Range of Motion	40

7	Part A Conclusion	41
7.1	Summary	41
7.2	Contributions.....	41
7.3	Future Work.....	41
Part B: Passive Ankle-Foot Orthosis (AFO) with Adjustable Assistance		
8	Background	44
8.1	Ankle Kinematics.....	44
8.2	Ankle-Foot Orthoses (AFOs).....	45
8.3	Relevance to Field.....	45
9	Literature Review	47
9.1	Solid Ankle-Foot Orthoses (SAFO).....	47
9.2	Posterior Leaf Spring Ankle-Foot Orthoses (PLS AFO)	48
9.3	Unpowered Exoskeleton	49
9.4	Pneumatic Muscle Ankle Exoskeleton	50
10	Design Criteria	53
10.1	Weight.....	53
10.2	Stiffness.....	53
10.3	Fast AFO Modification	53
10.4	Range of Motion	54
10.5	User Comfort	54
11	Design Concepts	56
11.1	Prototype.....	56
11.2	Final Design.....	57
12	Design Validation	60
12.1	Weight.....	60
12.2	Quantify Stiffness	60
12.3	Fast AFO Modification	66
12.4	Time to don and doff AFO.....	67
12.5	Natural Ankle Angle Interference.....	67
12.6	Comfort.....	67
13	Part B Conclusion	69
13.1	Summary.....	69
13.2	Future Work.....	69
14	Conclusion	71

List of Tables

Table 1: Hip Exoskeleton Engineering Requirements	26
Table 2: Component Weight for Hip Exoskeleton.....	36
Table 3: AFO Engineering Requirements.....	55

List of Figures

Figure 1: Body Planes & hip movement [28]	5
Figure 2: Hip kinematics during differing walking speeds [31]	6
Figure 3: Frontal Plane Joint angles for control male (dark blue) and control females (yellow). a) ankle inversion and eversion, b) knee adduction and abduction, c) hip adduction and abduction, and d) pelvis rotation to the same side and opposite side of subject’s stance leg. [35].....	6
Figure 4: Definition of human gait cycle [29]	7
Figure 5: Natural hip moment for individuals with CP [41]	8
Figure 6: Samsung Institute of Technology Hip Exoskeleton. 1) BLDC Motor, 2) joint actuator,, 3) passive hinge for abduction/adduction, 4) hip brace, 5) thigh frame, 6) spring loaded sliding mechanism, 7) CPU and battery [39].....	11
Figure 7: HONDA Automated Stride Assistance System A) Device A: Automated Stride Assistance System prototype [51], B) Device B: Stride Management Assist (SMA) System [52], C) Device C: Stride Management Assist Device [20], [53].	13
Figure 8: Hip components of the Berkeley BLEEX Exoskeleton [54]	15
Figure 9: a) PH-EXOS Design, b) Schematic of the Bowden cable actuation system [47].....	17
Figure 10: APO Device, a) device relative to user from different angles, b) device schematic: (1) Rear connecting bar, (2) Detachable pin for regulation, (3) fine adjustment lead screw, (4) rails for flexion-extension axes, (5) back support interface, (6) adjustment screw, (7) thigh frame, (8) thigh cuff, (9) sliding and rotational adjustment for thigh cuff, (10) passive abduction-adduction rotational axis [43] ..	18
Figure 11: University of Utah's hip exoskeleton. a) front and side views of unilateral hip exoskeleton, b) actuation system, c) above-knee amputee subject wearing the hip exoskeleton [57].	19
Figure 12: Harvard Exosuit [21]	22
Figure 13: Ankle-Hip Soft Exosuit. Anchor joint anchor points (blue), hip joint anchor points (red) [49]	23
Figure 14: Hip Exoskeleton Design. 1) Chain and Sprocket, 2) Motor, 3) Motor Case, 4) Bowden Cable, 5) Waist Belt, 6) Pelvic Hinge, 7) T-bar, 8) Pulley and Torque Sensor Assembly, 9) Joint Hinge, 10) Carbon Fiber Upright, 11) Thigh Cuff.....	28
Figure 15: Prototype B: (1) Motor Assembly, (2) Bowden Cables, (3) Waist belt, (4) Pelvic hinge, (5) T-bar, (6) Upper upright, (7) Torque sensor and pulley assembly, (8) Hip joint hinge, (9) lower upright, (10) Thigh Cuff, (11) cuff sliders	30
Figure 16: (A) Pelvic Hinge, (B) Hip Joint Hinge	31
Figure 17: Pelvic hinge and upright schematic	31
Figure 18: Final hip exoskeleton design. (1) motor assembly, (2) Bowden cables, (3) hip frame slider, (4) hip frame, (5) aluminum hinge, (6) T-bar, (7) upper upright, (8) torque sensor and pulley assembly, (9) lower hinge, (10) lower upright, (11) thigh cuff sliders, (12) thigh cuff.	32
Figure 19: Finite element analysis of pelvic hinge. (A) Loading conditions, (B) Results of stress deformation	33
Figure 20: Hip Exoskeleton torque testing trial. Blue indicates torque measured through the torque sensor at the hip joint, red represents the desired torque.	37
Figure 21: Hip exoskeleton protrusion distance	39
Figure 22: Ankle kinematics during differing walking speeds [31].....	44
Figure 23: Solid Ankle-Foot Orthosis [14]	47
Figure 24: Posterior Carbon Fiber Leaf Spring AFO [61].....	48

Figure 25: Passive Unpowered Ankle Exoskeleton [60]	50
Figure 26: Artificial pneumatic muscle powered ankle exoskeleton. (a) single muscle, (b) dual parallel muscle [70].....	51
Figure 27: Dual artificial pneumatic muscle for dorsi and plantarflexion assistance [71].....	52
Figure 28: Prototype for AFO Device. (1) upright, (2) plantarflexion assist leaf spring, (3) shin cuff, (4) upright slider, (5) ankle pulley, (6) torque sensor, (7) footplate	56
Figure 29: Final AFO Design. (1) upright, (2) cuff sliders with tightening cam mechanisms, (3) calf cuff, (4) plantarflexion assist leaf spring, (5) dorsiflexion assist leaf spring, (6) upright slider with tightening cam mechanism, (7) ankle pulley, (8) pulley-to-footplate adapter, (9) footplate	58
Figure 30: Reinforced Pulley Geometry. A) deformed prototype pulley, B) new proposed pulley design	59
Figure 31: Theoretical stiffness for 3 thickness of leaf springs	62
Figure 32: Beam stiffness testing jig.....	63
Figure 33: Three thickness leaf springs evaluated at different lengths to determine torque per rotation relationship for AFO stiffness evaluation	64
Figure 34: Theoretical and experimental data for 1/8" leaf spring	65

1 Introduction

1.1 Movement Impairments

Neurological conditions such as Cerebral Palsy (CP) can affect an individual's muscle control, resulting in reduced mobility and inefficient walking patterns. [1], [2]. Metabolic cost of transport (MCoT) is used to determine the efficiency of an individual's walking style; a more efficient gait cycle results in a lower MCoT.

CP is a permanent, nonprogressive, neurological birth defect that affects movement, muscle activation, and posture [3]–[5], making it more difficult to complete everyday tasks. It is the most common cause of pediatric physical disability [1], [4], [6] affecting 2-3 children for every 1,000 births [4]. Due to reduced muscle activation and lower mobility rates, CP has been shown to increase the MCoT by 2-3 times compared to unimpaired individuals [2], [7], [8]. Currently, there are no known cures for this condition, but there are extensive treatments to help maintain and improve quality of life such as physical therapy, orthotics, orthopedic surgery, and locomotion training [1], [6].

1.2 Treatments

To address movement impairments, physical therapists commonly prescribe orthotics, gait training, and physical therapy to help stretch and strengthen certain muscle groups. Orthopedic surgery is required for some severe cases of CP, but surgery is an expensive and invasive type of treatment requiring a long recovery for the child [6].

Physical therapy is a non-invasive, preventative type of treatment and is used to help individuals strengthen and stretch muscle groups that may have reduced mobility. Another common treatment option includes the use of orthotic devices, which can often be expensive depending on the type of orthotic required. Children grow rapidly, meaning their orthotics will

constantly need resizing. Ankle-foot orthoses (AFOs) are commonly used orthotics to correct ankle biomechanics for individuals with drop-foot or weak plantarflexor muscles, but they restrict ankle movement leading to reduced ankle power [1], [6], [9]–[14].

Locomotion training allows individuals to walk with assistance and has shown promising effects for children with CP. Several studies showed children that took part in locomotion training on a treadmill had improved hip extension, gait speed, step length, and overall gait functionality [15], [16]. Another locomotion training technique utilized in recent years includes exoskeletal devices, which are robotic devices worn on the outside of the body that assist the user with specific tasks [17]. Exoskeleton gait training teaches efficient walking patterns in parallel to treadmill training by gently guiding the individual into an efficient walking pattern. [1], [6], [15]–[18].

Several exoskeletons such as HAL [16], the Lerner Exo [19], and the Gait Trainer I [15] focused studies specifically on helping individuals with CP. Several other exoskeletons such as HONDA [20], the Harvard Lab [21], and Samsung Institute of Technology [22], have focused on stroke patients, individuals with muscle weakness, or generally improving a healthy individuals' MCoT.

Since individuals with CP are pre-exposed to reduced mobility, it is hard for these individuals to stay active, which is why it is important to promote an active lifestyle. According to a sports rehabilitation program, inactivity in individuals with CP due to aging and weight gain can lead to reduced aerobic capacity [23], which is why it is important to address movement disorders in children as early as possible [2], [24].

Both AFOs and exoskeletons have one common goal – to correct joint biomechanics and increase walking efficiency in individuals with movement impairments. Current AFO technology

reduces ankle motion, decreasing ankle power as a tradeoff to correct ankle biomechanics [14]. Rehabilitation exoskeletons show promise in gait training, but lack assistance for all joints in specific patient populations [19], [25]–[27]. The combination of an adaptive AFO and lightweight hip exoskeleton will augment human motion during walking – ultimately leading to reduced MCoT.

Part A: The Design and Validation of a Powered Hip Exoskeleton

2 Background

2.1 Hip Kinematics

The hip joint has 3 degrees of freedom (DOF) with movement on all three anatomical planes. Flexion and extension are defined by the forward and backward movement that happens on the Sagittal plane, shown in Figure 1. Abduction and adduction movement is defined as the side-to-side movement on the Frontal Plane. Internal and external rotation is defined by the leg rotation on the transverse plane.

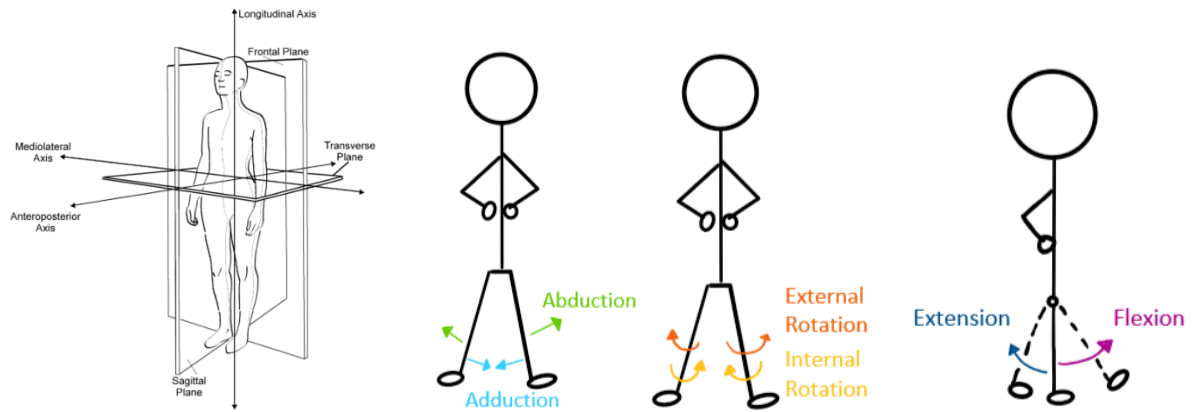


Figure 1: Body Planes & hip movement [28]

During level ground walking, the main form of movement in the hip is flexion and extension. For a healthy individual, the hip joint is expected to have a natural range of motion (ROM) of about 50° in the Sagittal plane; 35° in flexion and 15° in extension [29]–[34]. The different lower extremity joint angles during different walking speeds can be seen in Figure 2.

The hip joint torque for a healthy adult is expected to be $1.0 \frac{\text{Nm}}{\text{kg}}$ for extension and $0.9 \frac{\text{Nm}}{\text{kg}}$ for flexion, which is discussed more in depth in Chapter 2.2. Figure 2 indicates walking speed and joint moment are related. A faster walking speed means larger ROM and similarly, larger joint moment. It is important to note that for individuals with movement impairments such as

CP, muscle weakness, or stroke recovery, walking speeds are less than a healthy adult, indicating lower joint moments. The joint angle and moment are not expected to meet the same magnitudes for that of a healthy adult, however they should have a relatively similar profile.

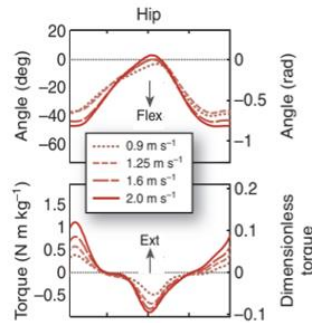


Figure 2: Hip kinematics during differing walking speeds [31]

Because the hip has multiple DOF, hip abduction/adduction and internal/external rotation need to be considered. During normal walking, the hip abduction and adduction angles as seen in Figure 3 Part c show that the maximum adduction to be about 8° and maximum abduction to be about 4° for a total of 12° during normal walking conditions for an unimpaired individual.

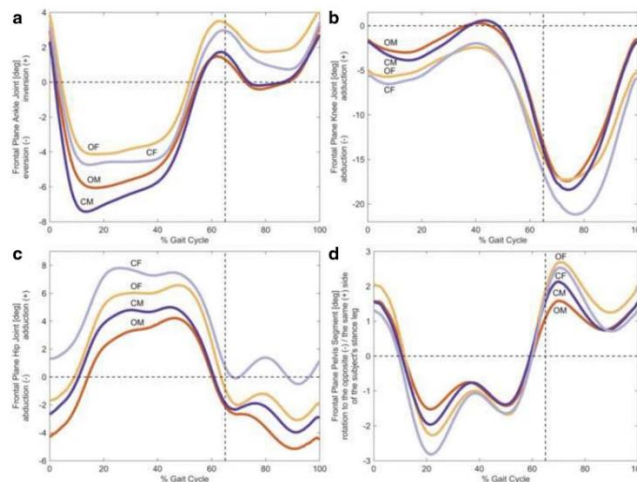


Figure 3: Frontal Plane Joint angles for control male (dark blue) and control females (yellow). a) ankle inversion and eversion, b) knee adduction and abduction, c) hip adduction and abduction, and d) pelvis rotation to the same side and opposite side of subject's stance leg. [35]

2.2 Kinematics for Impaired Individuals

Previous studies in Northern Arizona University's (NAU) Biomechanics Research Lab focused on improving mobility for children with CP. Children with CP are shown to have larger hip and knee flexion during their unassisted gait cycle, requiring more hip and knee extensor muscle effort [2]. A gait cycle is shown below in Figure 4 indicating peak extension occurs during early stance, and peak flexion during early swing. Hip extension torques during natural walking for an unimpaired individual reach up to $1.0 \frac{\text{Nm}}{\text{kg}}$ and peak at about 10% of the gait cycle. Likewise, hip flexion torques reach up to $0.9 \frac{\text{Nm}}{\text{kg}}$ and peak at about 60% of the gait cycle [31], [32], [34], [36]–[40].

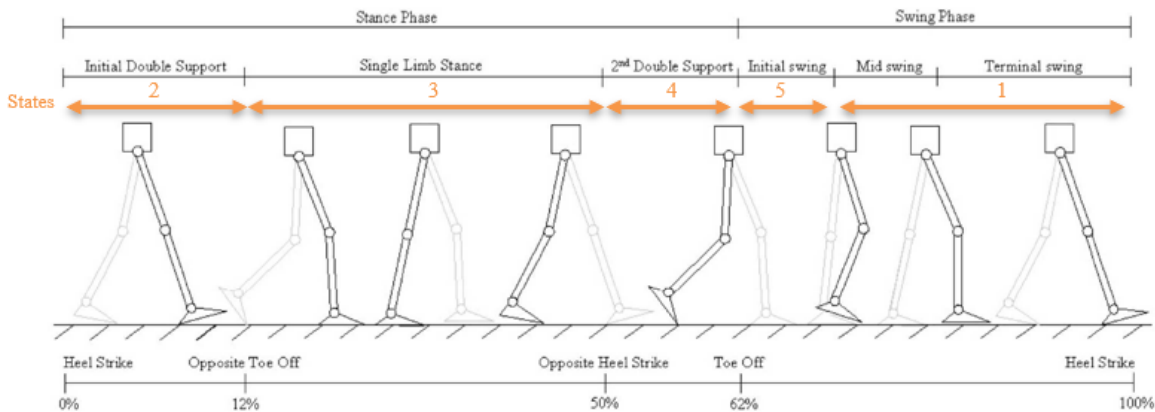


Figure 4: Definition of human gait cycle [29]

Figure 5 shows results from Lerner et al, indicating that children with CP on average have significantly smaller hip moments than unimpaired individuals, peaking at about $0.3 \frac{\text{Nm}}{\text{kg}}$ for flexion, and less than $0.1 \frac{\text{Nm}}{\text{kg}}$ for extension [41].

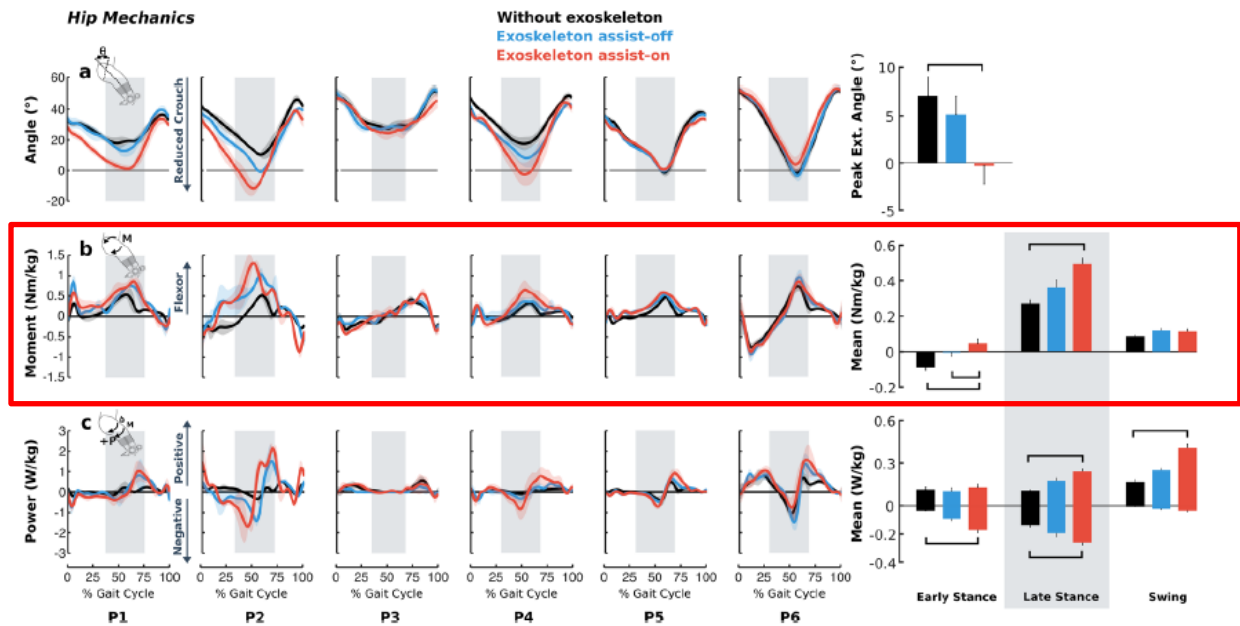


Figure 5: Natural hip moment for individuals with CP [41]

Powered exoskeleton training has been shown to reduce user muscle activation and therefore reduce the overall energy expenditure during physical activities [8], [42]. This allows the individual to learn more efficient walking techniques [15] while decreasing their MCoT. To train a more efficient walking gait, a hip exoskeleton could be used to apply an assistive torque at the hip joint during the extension and flexion phase of the gait cycle to help reduce MCoT.

2.3 Relevance to Field

Most hip assistance devices are designed for adult individuals with muscle weakness such as the elderly population or stroke patients [20], [22], [39], [43]–[46], but there are currently no powered, untethered, hip-only exoskeleton devices specifically for assisting children with movement disorders. Most exoskeleton devices for children with CP assist the ankle with plantarflexion [19], [25] or assist with knee extension [26], [27]. That said, as children with CP

have a high MCoT, it is important to address all areas of potential improvement to help keep them active throughout their childhood.

Inefficient joints such as the hip joint require more energy to actuate than the ankle joint due to energy storage within the tendons. Assisting inefficient joints can result in larger decreases for MCoT when compared to efficient joints by supplementing the tendons' energy loss [39]. Providing joint assistance at the hip is expected to significantly reduce the MCoT for a child with CP given the exoskeleton has adequate power to overcome the added mass of the device. Decreasing the overall MCoT would allow the child to train for longer periods of time more consistently without experiencing exhaustion due to their inefficient natural gait.

2.4 Exoskeletons

Exoskeletons are defined in this application as wearable robotics that operate and have close interaction with the human user, assisting with specific tasks such as increasing strength, assisting with rehabilitation recovery processes, and overall assisting with human movement operations [17]. There are three common types of exoskeletal devices that are used in research: rigid exoskeletons, soft exoskeletons, and pneumatic muscles.

Rigid exoskeletons are made of hard, durable, materials such as titanium, aluminum, or carbon fiber and require physical joints to be built into the device for the user to have natural movement. They are known for being durable and are used in high torque applications such as load carrying assistance. It is imperative that the exoskeleton shadows the users joints to operate synergistically with the user, or there is risk of hurting the user [47], [48].

Soft exoskeletons are made of fabrics and soft textile materials. These exoskeletons function by pulling two points – located above and below the joint – together to create a torque about the joint center of rotation. These types of exoskeletons tend to be lighter and smaller

profile when compared to the rigid types of exoskeletons, but they lack high torque capabilities due to the angled force applied to the lever arm [21], [49], [50].

Pneumatic muscles are mesh-like tubes that are placed parallel to the muscle or tendon requiring assistance. When the tube is inflated with air, the pneumatic muscle shortens, applying a force to the user. These exoskeletons require an air compressor connection and are loud to operate. Due to the nature of pneumatic muscles being tethered, loud systems, I will not be considering a pneumatic muscle design for my hip exoskeleton [32], [34].

The next section of this thesis will investigate rigid and soft exoskeleton systems in the literature to determine design successes and shortfalls. That information will then be used to discuss design parameters for the hip exoskeleton in Chapter 4 and design process in Chapter 5. Design validation will then be discussed in Chapter 6 to ensure the device meets the design parameters.

3 Literature Review

The following chapter discusses recent advancements in hip exoskeleton design and control systems. Each device was examined for specific mechanical features including actuation, transmission system, weight, ROM, and effectiveness. The following information was used to determine an optimal design for the first version of the hip exoskeleton.

3.1 Rigid Exoskeletons

3.1.1 Samsung Institute of Technology GEMS Device

The Samsung Institute of Technology developed a rigid, low profile hip exoskeleton specifically for assisting the elderly population with muscle weakness. Their goals were to ensure the exoskeleton was low profile and comfortable enough to fit under pants, lightweight to allow reduction in metabolic cost of walking, adjustable for different sized users, and could assist with both flexion and extension of the hip [22], [39]. The design can be seen in Figure 6.



Figure 6: Samsung Institute of Technology Hip Exoskeleton. 1) BLDC Motor, 2) joint actuator, 3) passive hinge for abduction/adduction, 4) hip brace, 5) thigh frame, 6) spring loaded sliding mechanism, 7) CPU and battery [39]

The hip exoskeleton design used a direct drive motor located at the hip joint. This allows for minimal system losses through a transmission system, but limits where the motors can be placed. The device includes one powered DOF for hip flexion and extension assistance, and one passive DOF for hip abduction and adduction movement. The ROM for flexion and extension is

120° and 45° respectively, and ROM for abduction and adduction is 20° in both directions. To account for the kinematic misalignment between the hip joint and the thigh frame, a spring-loaded slider was used to adjust the height of the exoskeleton leg to match that of the user during abduction and adduction movement. The exoskeleton thigh frame was made from plastic and carbon fiber to allow proper stiffness of the device during torque application while also allowing natural movement [22], [39]. The system had a total weight of 2.8 kg [39].

An open loop control system was used for this device, which relied on walking speed provided by an IMU located on the back, user weight, and hip angle to estimate the gait phase which then determined how much assistance torque to apply to the user. This system has a maximum torque of about 12 Nm [39].

This study concluded there was a MCoT reduction of $13.2 \pm 4.3\%$ per body mass while using assistance, indicating the device decreased energy expenditure while walking in the elderly population [39].

The GEMS device was relatively lightweight and included a large ROM for user comfort. However, this device utilizes a direct drive design, while the torque application may be effective without a transmission system, the location of the motor increases distal mass of the design increasing energy expenditure while walking. A motor located at the hip joint also increases the lateral protrusion distance, which can lead to discomfort and balance issues.

3.1.2 HONDA Device

The Stride Management Assist Device (SMA) developed by HONDA was designed to assist patients with weakened muscles such as the elderly population as well as recovering stroke and spinal cord injury patients. Several studies were completed with three types of the SMA devices.

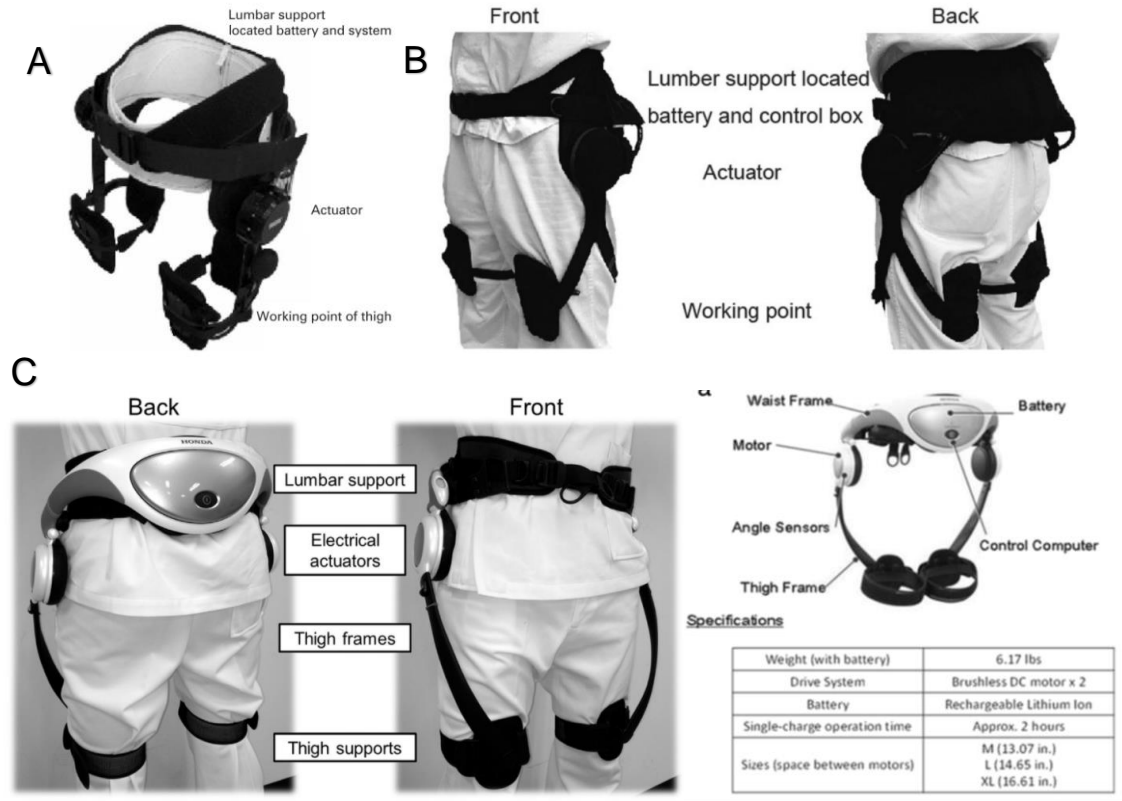


Figure 7: HONDA Automated Stride Assistance System A) Device A: Automated Stride Assistance System prototype [51], B) Device B: Stride Management Assist (SMA) System [52], C) Device C: Stride Management Assist Device [20], [53].

The first device shown in Figure 7a, will be referred to as Device A. Device A was used in a study to determine the change in muscular glucose metabolism in elderly adults. This device had angle sensors to determine cadence, velocity, and joint angles. The total weight of Device A was 3.5 kg, having a bi-directional actuator on both hips positioned at the joint center of rotation. Device A was specifically developed to improve gait endurance of elderly individuals with shortened strides through learning efficient walking techniques. The study concluded that the walking ratios, speed, stride lengths, and cadence of all subjects improved significantly without increasing lower-extremity muscle energy consumption [51].

The second device shown in Figure 7b will be referred to as Device B. This device was designed to assist older individuals improve their walking speed, step length, and walking patterns. Device B was equipped with angle sensors that monitored cadence, angular velocity,

and joint angles. The entire system weighted 2.4 kg with bi-directional actuators located at the hip center of rotation. The main differences between Device A and Device B are system weights and overall low-profile design. Device A has a bulky interface waist interface with larger motor mounts. Device B has a lower profile design consisting of a smaller waist strap, lower profile actuators, and lower profile thigh frames while being more than 1 kg lighter in overall mass. Much like the previous study with Device A, Device B also showed significant improvement in walking speed and decreased glucose metabolism in main lower-extremity muscles, making this assistive device useful in improving walking performance of the elderly population [52].

The third device shown in Figure 7c will be referred to as Device C. This is the final iteration of the HONDA device. Device C was designed for individuals with movement disorders to help improve walking performance [20]. The entire system with the battery weighed 2.8 kg and could be used for approximately 2 hours before battery depletion. The device had 2 low profile bi-directional actuators located at the hip joint center of rotation. The studies for Device C looked at improving walking speed and reducing glucose metabolism in lower limb muscles. The first study concluded the net metabolic cost of transport decreased by 7-10.5% in healthy young individuals with torque applications of about 4 Nm [53]. The second study included recovering stroke patients and concluded similar findings as found from device A and B [20].

The control system for the HONDA devices included a rhythm scheme that mimicked neural networks – which are responsible for rhythmic walking – by supplementing with a Central Pattern Generator (CPG). The CPG allowed the device to synchronize its movement with the user's movement. The torque application was then applied at specific points within the gait cycle by measuring the hip angle and walking patterns. The extensor torque was initiated after initial

contact and reached a peak just before mid-stance whereas the flexion assistance torque started during terminal stance and reached a peak around initial swing [20].

The three HONDA devices all include direct drive motors, similar to the GEMS device. While device B was lighter than the GEMS device, these designs all have similar issues including large protrusion distances, and increased distal mass.

3.1.3 BLEEX

Berkeley developed a full lower extremity exoskeleton assisting the hip, knee, and ankle joints designed specifically for heavy object lifting and military transport of heavy payloads. Because this thesis is only focused on assistance at the hip joint, I will only be discussing the designs of this exoskeleton that relate to hip assistance. The exoskeleton, nicknamed BLEEX, has 3-DOF at the hip: abduction/adduction, internal/external rotation, and flexion/extension. A simplified diagram exoskeleton is shown Figure 8.

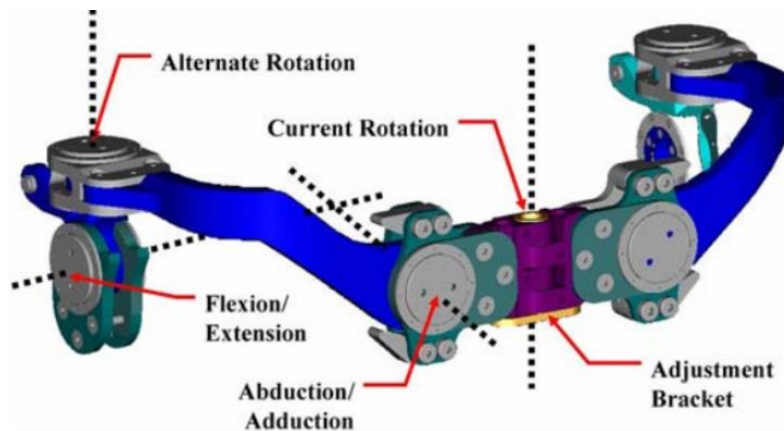


Figure 8: Hip components of the Berkeley BLEEX Exoskeleton [54]

The flexion/extension joints and abduction/adduction joints pass directly through the user's center of rotation whereas the internal external rotation was simplified to one axis located near the users back. Through experimentation, they determined if all 3 DOF were through the hip

joint, the ROM would be more limited. BLEEX maximum ROM for hip flexion and extension was 121° and 10° respectively. The ROM for hip abduction and adduction was 16° and 16° respectively. BLEEX maximum range of motion for total internal and external rotation was 35° and 35° respectively. BLEEX has two powered joints – flexion/extension and abduction/adduction – and two passive joints for internal/external rotation. BLEEX is one of the few exoskeletons that has powered frontal plane assistance due to balancing large payloads [54].

BLEEX is one of the few exoskeletons that is actuated through a hydraulic system. Hydraulic systems are generally used for heavy duty tasks due to their durable and heavy nature. Since BLEEX is a full lower extremity exoskeleton with a rigid frame spanning from the sole of the shoe to the hips, it is self-supporting. This takes a significant load off the user as the weight of the machine is in direct contact with the ground and in no way would impede the user's energy consumption [54], [55].

BLEEX's control system was closed loop, with each joint including an encoder and linear accelerometer to determine joint angle, angular velocity, and angular acceleration. The controller does not have any interaction forces with the human body and estimates movements with force sensors located on the joint actuation units. This causes the exoskeleton to be susceptible to outside forces not provided from the user [54].

3.1.4 PH-EXOS

The PH-EXOS is a hip-only exoskeleton that uses Bowden cable transmission to actuate the hip joint through motors not located at the center of rotation. A diagram of the design can be seen in Figure 9. PH-EXOS is a 3-DOF system with 2 passive DOF in the frontal and transverse planes for abduction, adduction, internal rotation, and external rotation, and 1 powered DOF in the sagittal plane for flexion and extension. This exoskeleton uses 2 AC servo motors that are

mounted to the back of the device, requiring a transmission system to allow the torque to be applied directly to the hip center of rotation. The total weight of the exoskeleton is 3.5 kg. The design accounts for changes in length of the exoskeleton leg with respect to the user by implementing a slider unit near the thigh cuff, allowing more natural movements and comfort for the user [47].

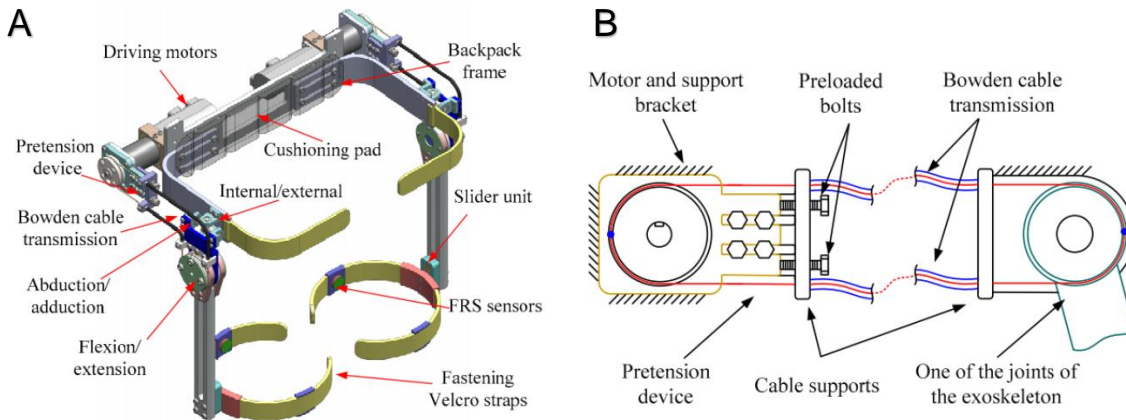


Figure 9: a) PH-EXOS Design, b) Schematic of the Bowden cable actuation system [47]

The PH-EXOS control system includes force sensitive resistors (FSRs) on the thigh braces to measure the interaction forces and motion intention of the user. The exoskeleton operates using a cascaded proportional-integral-derivative (PID) controller to track trajectory and respond quickly to the user. The exoskeleton uses FSRs located in the thigh cuffs as inputs to the system which are then run through a fuzzy adaptive controller to be used in the PID controller to change the motor actuation based on the user's movements [47].

Shortfalls of this device include an uncomfortable hip brace, and the large system weight. The devices' hip brace is a rigid square frame that does not connect securely to the user in a comfortable fashion, and the large ROM increased the number of parts in the device, increasing the device weight. An increased device weight is correlated to increased MCoT [56].

3.1.5 Lightweight Active Pelvis Orthosis (APO)

The APO device is a hip-only powered exoskeleton made from carbon-fiber arms with bi-directional motors located at the hip joints. The entire system has 3 DOF and weighs about 4.2 kg. A schematic of the device can be seen in Figure 10. The thigh and rear frames are made from carbon fiber allowing the device to meet structural requirements while also maintaining a lighter weight. The APO uses DC motors coupled with harmonic drives and includes a series elastic actuator [43].

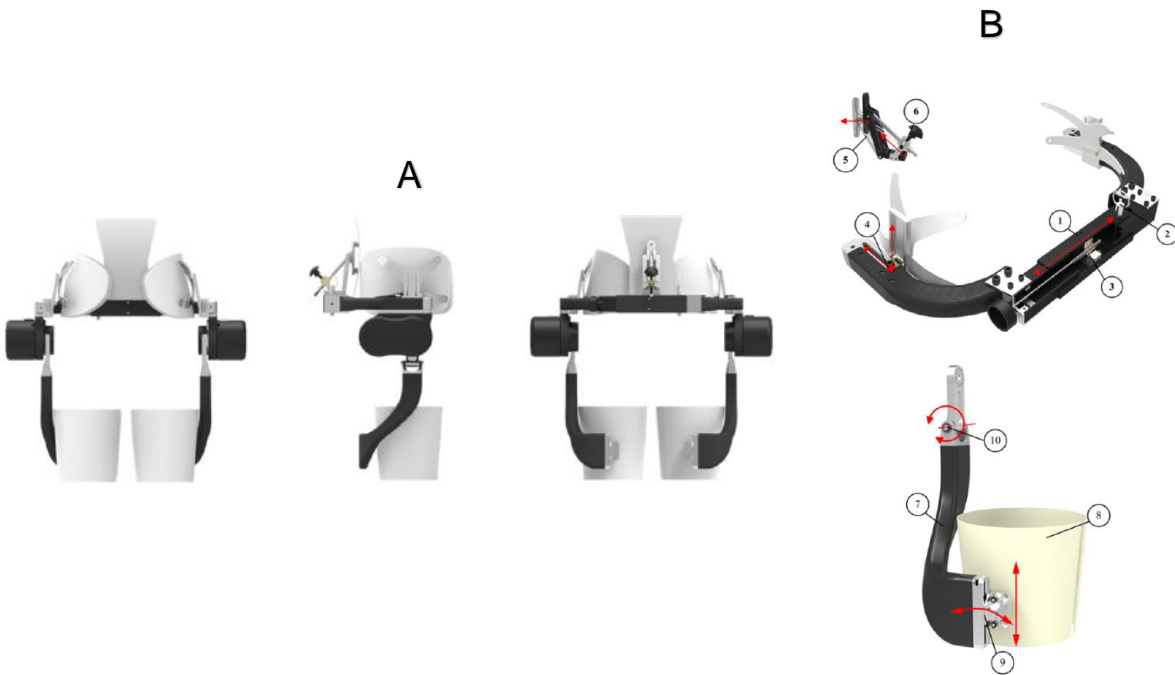


Figure 10: APO Device, a) device relative to user from different angles, b) device schematic: (1) Rear connecting bar, (2) Detachable pin for regulation, (3) fine adjustment lead screw, (4) rails for flexion-extension axes, (5) back support interface, (6) adjustment screw, (7) thigh frame, (8) thigh cuff, (9) sliding and rotational adjustment for thigh cuff, (10) passive abduction-adduction rotational axis [43]

The control system for the APO includes a low-level and high-level control. The low-level controller determines the torque value to send to the actuators, whereas the high-level control determines the desired torque based on the user's progress through the gait cycle. Deformation was measured in a torsion spring to determine the difference between the desired and measured torques in the system. The difference was then sent to a closed-loop PID controller

where the desired torque was modified. The high-level controller sends the desired torque based on the users position to the low-level controller which then determines actuator movement to supply the user with joint torque [43]. To determine the performance of torque control for this exoskeleton, the study computed the root means square error (RMSE) between the desired and measured torques. The RMSE value was $0.0029 \frac{\text{Nm}}{\text{kg}}$ for $0.55 \frac{\text{m}}{\text{s}}$ and an RMSE value of $0.0153 \frac{\text{Nm}}{\text{kg}}$ for $1.4 \frac{\text{m}}{\text{s}}$ in assistive mode.

The APO device included a large ROM for user comfort, however this device was heavy compared to others in the literature. This device included a direct drive transmission system, causing a large protrusion distance at the hip joint. This can cause issues during arm swing such as user discomfort if they collided with the device, balance issues, and potnetial device malfunction.

3.1.6 University of Utah's Unilateral Hip Exoskeleton

The University of Utah created a unilateral hip exoskeleton to assist above-knee amputees during walking. The exoskeleton can be seen in Figure 11.

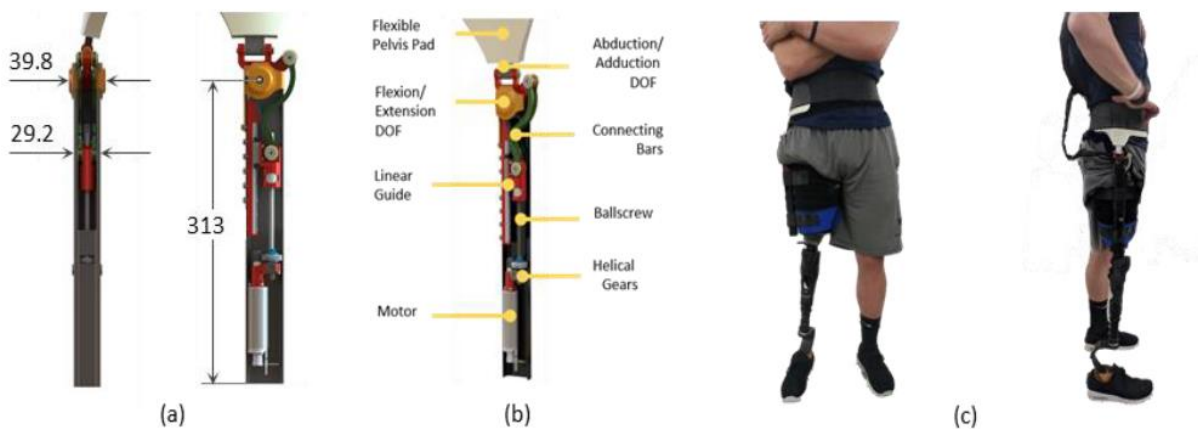


Figure 11: University of Utah's hip exoskeleton. a) front and side views of unilateral hip exoskeleton, b) actuation system, c) above-knee amputee subject wearing the hip exoskeleton [57].

The exoskeleton utilizes a carbon fiber tube that houses all actuator components, allowing the device to be lightweight and have a small protruding leg to avoid interference during arm swing. A Maxon DC motor was placed inside the carbon fiber tube, which then turned a ball screw through helical gear transmission to power the hip flexion and extension assistance. The exoskeleton included a passive hinge joint in series with the flexion/extension actuation to allow for the user to make abduction/adduction movements. The waist strap and thigh cuff were tightly fitted to the user's anatomy and were fabricated from polyurethane plastic to allow for flexible and comfortable use. The thigh cuff contained a slider mechanism to allow comfortable abduction and adduction movements due to the varying distance between the exoskeleton leg and the user's leg. The entire unilateral hip exoskeleton weighed 2.032 kg with a protrusion distance of 3.98 cm. This flexible lightweight hip exoskeleton can provide torques up to 45 Nm and can provide up to 81% and 94% of the nominal hip torque profile for a 90 kg able-bodied person [57].

The unilateral hip exoskeleton used a high and low-level control strategy. The high-level controller used an adaptive frequency oscillator to estimate the gait cadence and phase changes throughout the gait cycle. Hip assistance was then provided to the user at a specified phase in the gait cycle by actuating the motors through the low-level controller. Torque effectiveness was determined by fitting the phase estimate to a linear regression for ideal torque estimates and determining the RMSE. The unilateral hip exoskeleton had an RMSE value of 0.74% during assistive mode, indicating torque application was effective.

The University of Utah's unilateral hip exoskeleton was the lightest rigid exoskeleton with the largest torque application; however, this exoskeleton only had one leg, and the motors was located inside the tube making them hard to service. The placement of the motors also cause a

large protrusion distance at the hip and increased distal mass leading to similar issues experienced by the GEMS, HONDA, and APO devices.

3.2 Soft Exoskeletons

3.2.1 *Soft Exosuit*

The Harvard Biodesign Lab developed a different kind of exoskeleton free of hard materials and joint centers. This allows the device to apply torque at a specific joint by relying on the anatomy of the user. This specific device, seen in Figure 12, uses a soft textile material similar to seatbelt material that attaches to the back of the thighs. When the user heel strikes, the motors are actuated and start to wind the fabric around a spool, creating a force on the back of the thigh. At about 20% of the gait cycle, the force stops, and the material is unspooled so that the force sensors read zero. The Soft Exosuit is relatively large when compared to the user with an overall weight of 7.57 kg, but since most of the weight is located near the center of mass, the relative inertia is low making it more efficient to walk than a rigid exoskeleton of the same weight. Stated in the study, the Exosuit can contribute up to 30% of the nominal biological moment for walking, despite not having a perfectly perpendicular force applied to the thigh [21].

Issues with this design include the large weight located on the back of the user making it difficult to balance during walking. The exoskeleton only applied an extension torque during stance and had no flexion assistance, making the device unsuited to certain patient populations.



Figure 12: Harvard Exosuit [21]

3.2.2 Ankle-Hip Soft Exosuit

The Harvard Biodesign Lab created another lower extremity exoskeleton that assisted with both hip extension and indirectly assisted with hip flexion opposed to their previous design which just assisted with hip extension. The ankle-hip soft exosuit is tethered, meaning it must be physically connected to a stationary unit. The design can be seen in Figure 13 where the tethered Bowden cables are attached to the red anchor points for hip extension and another set of Bowden cables are attached to the blue anchor points for indirect hip flexion. The ankle-hip soft exosuit has direct assistance for hip extension similar to the previous Soft Exosuit, pulling the two red anchor points closer together. Hip flexion is indirectly assisted through assisting ankle plantarflexion, relying on toe off to propel the leg forward. When the system is actuated the cables shorten creating a force between the respective anchor points and effectively assisting the hip joint bi-directionally [49].



Figure 13: Ankle-Hip Soft Exosuit. Anchor joint anchor points (blue), hip joint anchor points (red) [49]

The exosuit had load cells located within the motor box to measure the Bowden cable tension and a gyroscope mounted to the back of the boot to determine the users progress within the gait cycle [49].

A large shortfall of this design was the need for a large actuator unit stationed close to the device. Without the actuator unit, the device could not function. Due to the untethered nature of this design, it would not be useful outside a strict lab setting.

4 Design Criteria

The hip exoskeleton was designed and validated for specific engineering requirements, outlined below, comparable to designs in the literature. The design criteria included requirements for weight, ROM, Torque assistance, and user comfort.

4.1 Bilateral-dual assistance

The hip exoskeleton will be bilateral with the goal of assisting individuals with hip flexion and extension while walking. It is important to assist the user in both swing and stance phases to ensure proper gait actuation.

4.2 Weight

It is important to minimize the hip exoskeleton weight to ensure the user's metabolic cost is not increased due to heavy load carrying. The hip exoskeleton will have a weight requirement of 2 kg for the entire system, comparative to weight of current hip exoskeletons in the literature. University of Utah's unilateral hip exoskeleton has a total weight of 2.032 kg, and the lightest bilateral hip exoskeleton in the literature was provided by HONDA at 2.4 kg.

4.3 Range of Motion

The hip exoskeleton must not restrict natural motion during level ground walking. This includes flexion and extension movement during assistance, and passive abduction and adduction movements for balance. If the exoskeleton impedes the natural range of motion of the user, the user will feel discomfort, torque application will not be as effective, and the user may have trouble balancing.

4.4 User Fit and Comfort

The hip exoskeleton will fit different sized users ranging from about 1.5 m to 1.8 m in height, assuming average body metrics. The exoskeleton will be comfortable for all users while walking. The user should comfortably be able to wear the hip exoskeleton for a minimum of 30 minutes with and without torque assistance. The exoskeleton will allow adjustment based on user metrics to fit securely around the waist and thigh.

4.5 Lateral Protrusion

The lateral side of the exoskeleton will have a low protruding profile to avoid contact during arm swing while walking. If the exoskeleton has a large protrusion outward, the user's arms may hit the exoskeleton, increasing user discomfort, affecting the users balance, and potentially affecting the assistance torque. A maximum protrusion distance for the exoskeleton will be less than 4 cm, comparable to the University of Utah's hip exoskeleton.

4.6 Torque Application

The hip exoskeleton will provide bidirectional torques of similar magnitude to those seen in the literature, with a low tracking error to ensure effective torque application. The maximum assistance torque for both flexion and extension should reach 12 Nm while having a tracking error of less than 10% for peak assistance.

All hip exoskeleton requirements are summarized in Table 1.

Table 1: Hip Exoskeleton Engineering Requirements

Requirements	Validation
Weight < 2kg	Weight entire system with scale
RMSE < 1.2 Nm	Collect data from a walking trial and calculate error.
Fit people 1.5 – 1.8 m tall (5-6 ft)	Measure minimum and maximum cuff sizes and waist circumference. Must fit in average body metrics for specific heights.
Comfortable rating ≥ 2	Have 3-5 volunteers of different heights and statutes try on device and rate comfort from 1-3. 1 = impossible to wear 2 = some discomfort in spots, but can be worn for 30 minutes 3 = extremely comfortable.
Protruding distance < 4 cm	Measure distance of the exoskeleton at the hip joint outward from the body on the frontal plane.
Range of Motion: Flex/Ext – 90/15 deg Abd/Add – 15/15 deg	Move exoskeleton to minimum and maximum positions and measure the angles.
Max torque >12 Nm	Measure applied torque to the user during the walking trial.

5 Design Concepts

The NAU Biomechatronics Lab currently has a powered ankle exoskeleton and a powered knee-ankle exoskeleton, both designed as rigid systems. The lab's rigid exoskeleton design was developed from the use of a closed loop control system requiring torque feedback from the exoskeleton joint. For compatibility, verification, and future project purposes, I designed the hip exoskeleton as a rigid system allowing parts to be compatible between the different exoskeletons, past and future. A rigid exoskeleton allowed for accurate torque readings and application to the user while also limiting range of motion for abduction and adduction directions to ensure the user does not over abduct or adduct during walking. A rigid system design allowed the hip control system to resemble a modified ankle exoskeleton control system from past devices to allow compatibility between systems.

5.1 Mechanical Design

5.1.1 *Prototype A*

The first prototype of the rigid hip exoskeleton was designed with three degrees of freedom for powered flexion and extension assistance, as well as passive operation for abduction and adduction movement. The powered flexion and extension assistance was actuated through steel cables housed in Bowden tubes. The Bowden cables spanned from motors located on the lower back to the exoskeleton joint center. The Bowden cable driven design allowed for heavy components – such as the motors – to be placed at an optimal location in the system for comfort and walking efficiency. When the motors actuated, it rotated the pulley located at the hip joint through the Bowden cable transmission, applying force on the thigh. Prototype A can be seen in Figure 14.

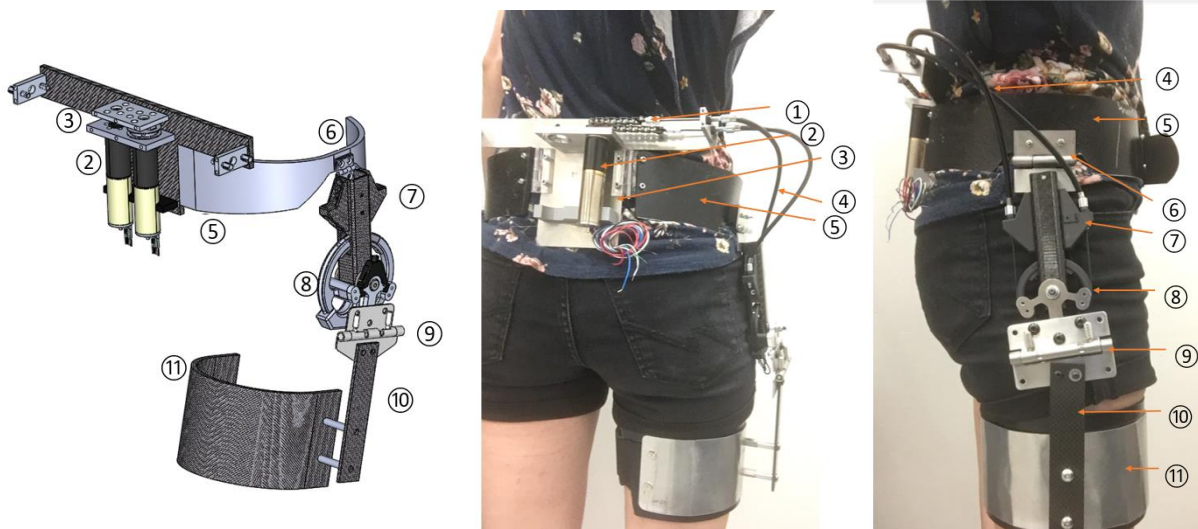


Figure 14: Hip Exoskeleton Design. 1) Chain and Sprocket, 2) Motor, 3) Motor Case, 4) Bowden Cable, 5) Waist Belt, 6) Pelvic Hinge, 7) T-bar, 8) Pulley and Torque Sensor Assembly, 9) Joint Hinge, 10) Carbon Fiber Upright, 11) Thigh Cuff

To account for natural hip movement, a two-hinge design was used: one located on the waist belt, and the other located at the hip joint. The hinge located on the waist belt accounted for different hip anatomies between participants. The hinge located at the hip joint accounted for abduction and adduction movement during walking or sitting.

The motor assembly included an aluminum plate with two motors oriented vertically and the drive shafts pointed upward. A chain and sprocket transmission system was used to transfer power from the motors to the steel cables. This design was proven effective in transmitting the power with minimal degradation in the system by a previous graduate student [56]. The steel cables then spanned the length of the Bowden tube until the Bowden cables terminated at the T-bars. The T-bars guided the steel cable into the pulley channel ensuring cable alignment during torque application.

The pulley and torque sensor assembly resembles the NAU Biomechatronics Labs' ankle exoskeleton. The pulley was manufactured using the Mark Forged II 3D printer, comprising of Onyx – nylon with chopped carbon fiber – and additional carbon fiber strands embedded into the

part during printing. The torque sensor was machined from 7075 T651 Aluminum manufactured by Protolabs and instrumented in house.

During testing of this prototype, future improvements were noted:

- The thermoplastic waist belt and thigh cuff would not fit more than one user at a time without remolding.
- The lower carbon fiber upright bar was flexible and allowed bending in the frontal plane.
- Both hinges included too much relative motion, affecting the accuracy of the torque readings.
- The Bowden cable path included sharp curvatures, affecting the efficiency of the transmission system.
- The motor assembly plate was uncomfortable on the back.
- The thermoplastic thigh cuff was flimsy and affected accurate torque readings.

5.1.2 Prototype B

Prototype B was manufactured to address issues with Prototype A. Prototype B included a fully updated motor assembly, newly manufactured pelvic hinges, and an updated thigh cuff assembly. The motor assembly resembled the ankle exoskeleton motor assembly from the NAU Biomechatronics Lab. The Bowden cables spanned from the top of the motor box to the top of the upper upright allowing the Bowden cable path to have a larger radius of curvature than the previous Prototype A. This provided more efficient power transfer through the cables due to lower friction between the steel cable and the Bowden sheath [58]. The updated design can be seen in Figure 15.

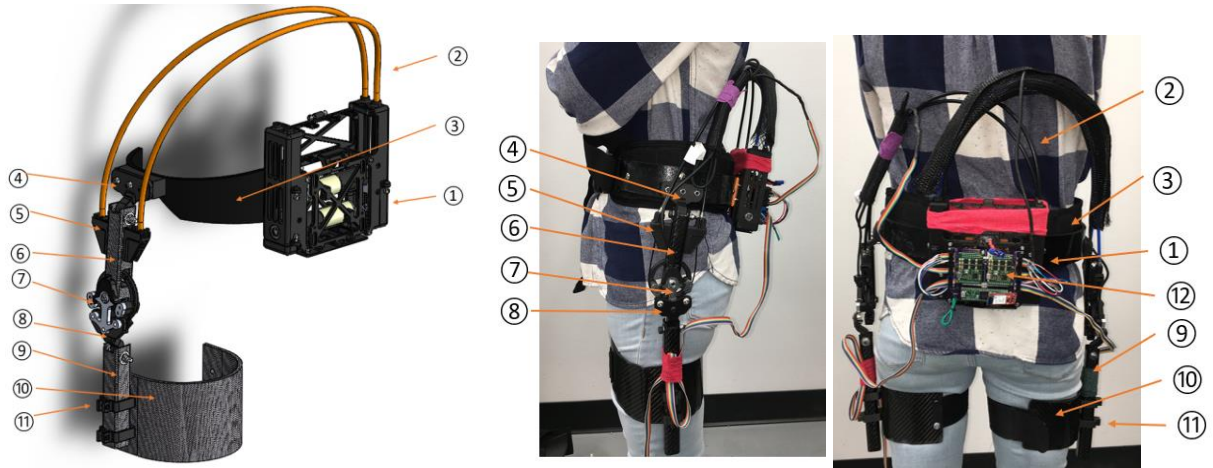


Figure 15: Prototype B: (1) Motor Assembly, (2) Bowden Cables, (3) Waist belt, (4) Pelvic hinge, (5) T-bar, (6) Upper upright, (7) Torque sensor and pulley assembly, (8) Hip joint hinge, (9) lower upright, (10) Thigh Cuff, (11) cuff sliders

To address previous concerns from Prototype A, the waist strap was manufactured out of thicker thermoplastic and attached to the motor assembly with two simple hinges. The simple hinges allowed the hip cuffs to be opened in a clam shell maneuver to allow users to put on the device and then closed to securely attach around the hips. The thigh cuff was updated to carbon fiber to help stiffen the user interface components, increasing the transmission efficiency. Additionally, the thigh cuff connection points were updated to sliders that easily slid over the lower upright, then secured in place, making it easy to replace. The lower upright was modified from a carbon fiber bar to a carbon fiber tube to avoid unwanted bending in the system.

The pelvic and hip joint hinges were updated to include different geometry which reduced the relative movement in the system. The pelvic and hip hinge designs can be seen in Figure 16.

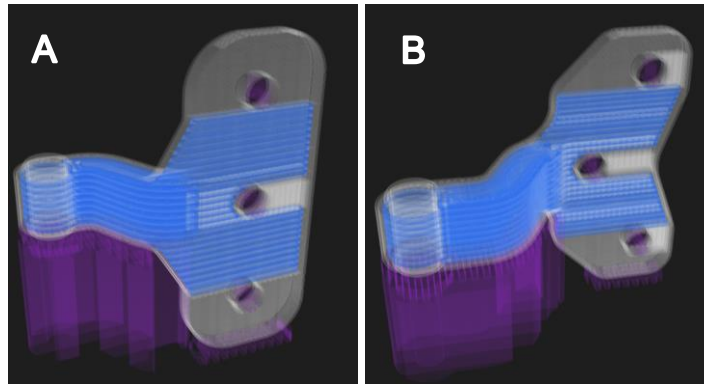


Figure 16: (A) Pelvic Hinge, (B) Hip Joint Hinge

The updated hinges were made from 3D printed Onyx and carbon fiber to strengthen the neck of the part and minimize excess movement. The embedded carbon fiber strands are indicated in Figure 16 as the blue shaded area. The barrel of the hinge was then placed inside the upright tube between two ball bearings with a shoulder bolt spanning the three parts to create the hinge, shown in Figure 17.

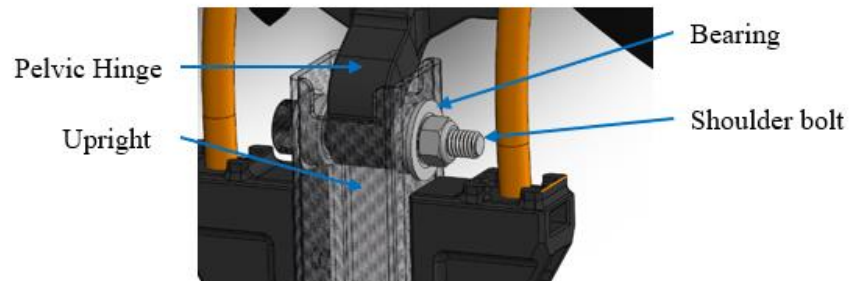


Figure 17: Pelvic hinge and upright schematic

During testing of Prototype B, future improvements were noted:

- Hip frame had excessive movement relative to the user, making it uncomfortable and affected torque tracking.
- The 3D printed Onyx/Carbon Fiber pelvic hinge deformed at high torques.
- The hip frame did not comfortably fit a large range of users.

5.1.3 Final Design

To address concerns with Prototype B, the final device was designed with universal features. The final design can be seen in Figure 18. The motor assembly was not modified from Prototype B. A new attachment piece was developed to attach the hip frame to the back of the motor assembly. The previous hip frame had two simple hinges that did not allow different sized users to comfortably wear the exoskeleton. The slider mechanism shown in Figure 18 Part 3 was designed to allow the hip frame to open by pulling the hip frames apart, and securely fastening around the user's waist by pushing them back together. This ensures the center of rotation of the hip exoskeleton is as close as possible to the user's natural hip joint, while being comfortable for a larger range of users.

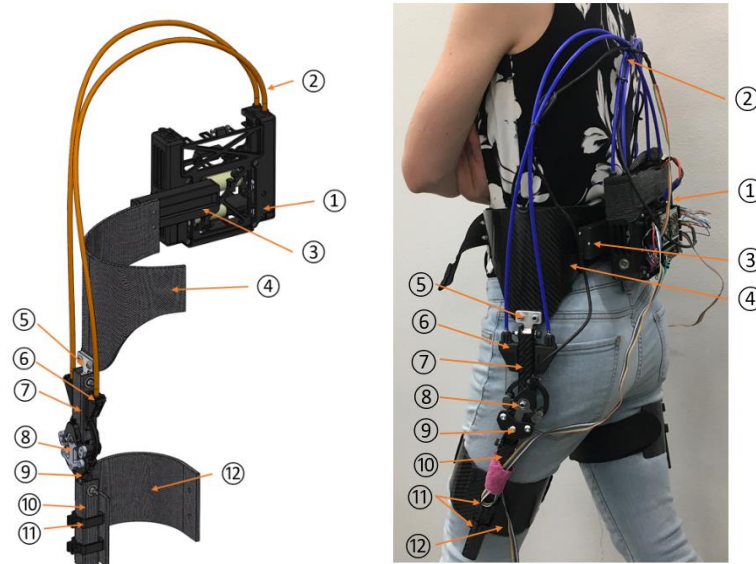


Figure 18: Final hip exoskeleton design. (1) motor assembly, (2) Bowden cables, (3) hip frame slider, (4) hip frame, (5) aluminum hinge, (6) T-bar, (7) upper upright, (8) torque sensor and pulley assembly, (9) lower hinge, (10) lower upright, (11) thigh cuff sliders, (12) thigh cuff.

The hip frame geometry was modified to help reduce movement between the exoskeleton and the user. Instead of a uniform hip frame seen in Prototype B, the final design utilized the natural geometry of the hip to ensure transmission efficiency was adequate and the exoskeleton connection points were comfortable by attaching around the waist with a portion spanning over

the hip. The hip frame design was inspired by the Bionic Engineering Lab’s hip exoskeleton due to their high torque capabilities with a hip frame made from flexible polyurethane [57].

To address issues with the 3D printed hinge at the hip frame interface, a new hinge was designed. The new design was smaller, made from aluminum, and did not have a protruding neck geometry. The hinge was made from 7075 T651 aluminum manufactured by Protolabs.

A basic finite element analysis (FEA) was completed using Solidworks to estimate the factor of safety (FS) during loading conditions. The part included fixed geometry at the bolt locations and an applied load at the bearing location resulting from torque application. FEA results can be seen in Figure 19 where (A) shows the loading conditions and (B) shows the stress results from the analysis.

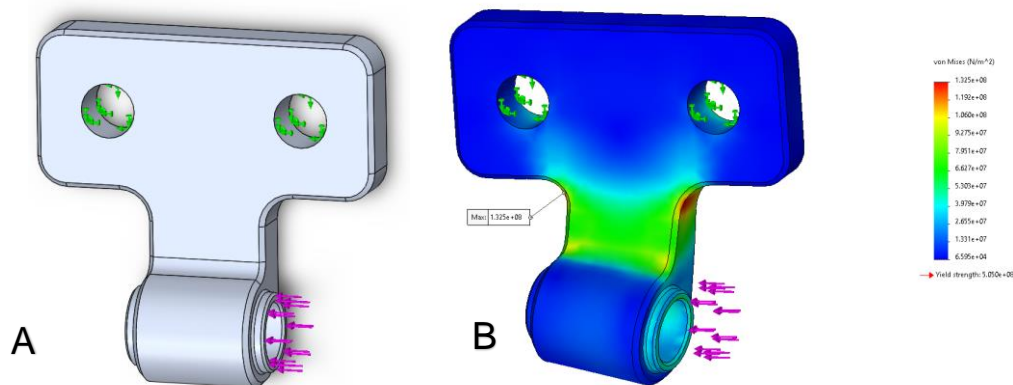


Figure 19: Finite element analysis of pelvic hinge. (A) Loading conditions, (B) Results of stress deformation

From the analysis, the stress concentration location occurred at the connection point between the neck and the face. Torque was simulated through force application at the bearing hole face equaling 750 Newtons, which was about 12 Nm of torque. The parts FS was 3.8, indicating the part will not plastically deform until torques exceed 45 Nm.

Results for the final design testing are discussed in Chapter 6: Design Validation.

5.2 Control System

The control system for the hip exoskeleton was developed by a PhD student working in the NAU Biomechatronics Lab. The PhD student developed previous control systems for the knee-ankle exoskeleton by modifying the control scheme for the previous ankle-only exoskeleton. The hip exoskeleton control system was developed in a similar manner, basing the foundation on the ankle-only and knee-ankle exoskeleton control systems. Two types of control systems were developed for the device – Bang-Bang and Proportional – to determine which control strategy was more comfortable and effective for torque application [19], [25].

5.2.1 *Bang-Bang*

Bang-Bang control is defined as being either on or off, has one set point, and does not react to changes in the gait cycle. The control strategy uses force sensitive resistors (FSRs) located in the shoe insole to determine the participants walking state – early stance, mid stance, late stance, or swing – which determines when assistance will be applied. Since natural flexion and extension hip torques for an unimpaired individual are about equal in magnitude, the control system provided flexion assistance during early swing (state 5), and extension assistance during early to mid-stance phases (state 2 and 3). See Figure 4 for state definitions in reference to the gait cycle.

When a torque was applied through the bang-bang control system, a desired torque value was sent to the motors. The motors actuated providing torque to the user in the specified direction. When torque was applied, the torque sensor recorded the value seen at the hip joint and relayed the measured torque value to a PID controller, where the value was adjusted and sent back to the motors to adjust. This repeated while the user was walking with the hip exoskeleton until the trial ended.

5.2.2 *Proportional*

Proportional control was different than the bang-bang control strategy by using FSR input to determine desired torque. Bang-bang control set one torque value and was either on or off and did not rely on FSR values. Proportional control instead used FSR inputs to proportionally apply torque to the user based on the FSR readings. The higher the FSR reading, the larger the desired torque. This controller was used to help make torque application more sensitive to user input throughout the gait cycle and overall made it more comfortable for the user when compared to bang-bang control.

The closed loop control system for bang-bang and proportional operated similarly, applying a desired torque to the user, measuring the actual torque, and refining the torque value through a PID controller.

6 Design Validation

To validate the mechanical design of the hip exoskeleton, engineering requirements from Table 1 were tested. Seven engineering requirements were validated: weight, torque tracking, torque magnitude, user fit, comfortability, protruding distance at the hip, and range of motion of the hip joint.

6.1 Weight

Components of the bilateral hip exoskeleton were weighed and summarized in Table 2. The hip exoskeleton had a total weight of 2.1 kg, 1.96 kg without the battery, satisfying the weight requirement. The proposed hip exoskeleton design is comparable to others in the literature such as the University of Utah's unilateral hip exoskeleton weighing a little over 2 kg [57], Samsung Institute of Technology bilateral hip exoskeleton weighing 2.8 kg [39], and the HONDA bilateral hip exoskeleton weighing 2.4 kg [52].

Table 2: Component Weight for Hip Exoskeleton

Component	Weight (kg)
Motor Assembly + PCB board	1.01
Leg (x2)	0.71
Thigh Cuff (x2)	0.24
Battery	0.14
Total	2.10

6.2 Torque Tracking

To determine effectiveness of torque application for the hip exoskeleton, a torque tracking validation was required. The RMSE for a trial had to be less than 1.2 Nm, or 10% of the maximum torque. An example of the hip exoskeleton torque tracking can be seen in Figure 20 where the measured torque at the hip joint is in blue and the desired torque is in red. Torque validation used the proportional control system due to comfort preference from the user. The RMSE for 12 Nm torque assistance was 4.77 Nm, and the RMSE for 8 Nm torque assistance was 3.19 Nm. It can be noted that the torque tracking error decreased with lower assistance torque.

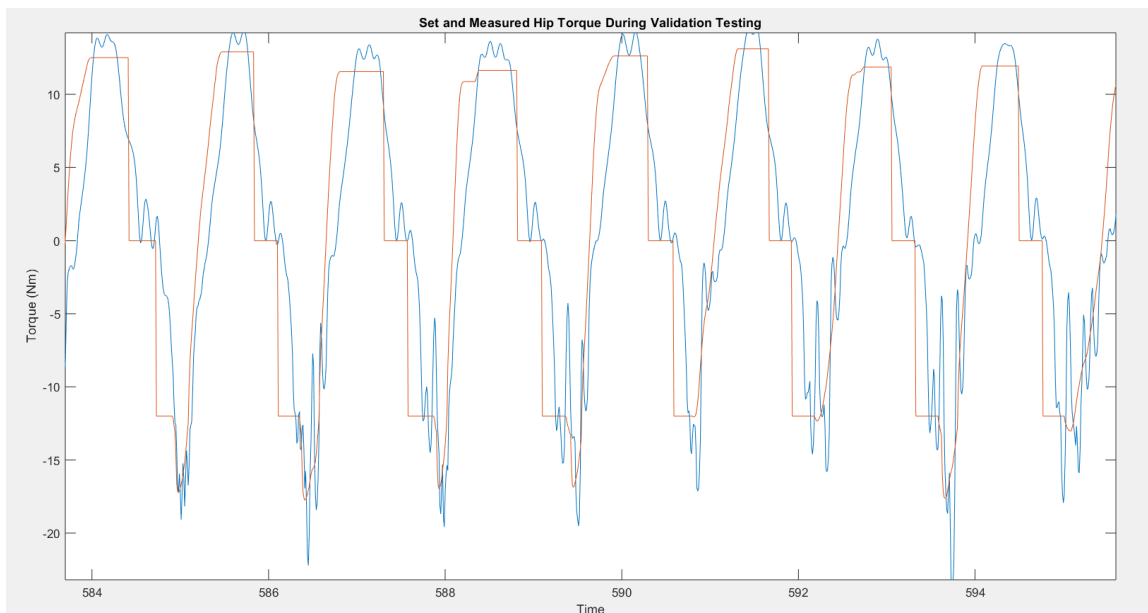


Figure 20: Hip Exoskeleton torque testing trial. Blue indicates torque measured through the torque sensor at the hip joint, red represents the desired torque.

Based on the validation data in Figure 20, the RMSE value calculated for 12 Nm of assistance torque did not satisfy the torque tracking requirement. The large RMSE value was much larger than expected and was believed to be caused by excessive noise in the measured torque readings. To reduce torque tracking error in future tests, the control system will be modified and PID control optimized to minimize noise in the system. The control system

currently applies the desired torque in steps and does not smooth the desired torque function to change gradually, causing larger errors when the torque setpoints change.

The aim of determining torque tracking error was to ensure the mechanical system could apply torque at the correct phase of the gait cycle. This was intended to be completed with RMSE, but due to excessive noise in the measured torque readings, the data was visually inspected. From Figure 20, the measured torque was compared to the desired torque for shape and magnitude. The measured torque followed the desired torque closely, peaking at the same times in the gait cycle. This visual inspection indicated minimal system losses due to torque responsiveness and timing within the gait cycle, satisfying the torque timing requirement.

6.3 Maximum Torque

To be effective for rehabilitation purposes, the hip exoskeleton had to reach a maximum torque of 12 Nm. Torque data collected during testing shown in Figure 20 indicate the hip exoskeleton reached a maximum torque of 14.6 Nm for extension and 24 Nm for flexion, satisfying the maximum torque requirement.

6.4 User Fit

To evaluate user fit, the hip brace was measured and compared to average body metrics for different aged users. The hip cuff has a minimum circumference of 78 cm and maximum circumference of 111 cm. A study found that average hip measurements for both males and females between the ages 7 and 17 ranged from 62 cm to 91 cm [59]. The thigh cuff has the ability to be switched quickly between users, where users can choose from 3 thigh cuff sizes ranging from small, medium, and large. From this data, the hip exoskeleton is expected to fit individuals aged 13 and older.

6.5 Comfort

To evaluate user comfort, three unimpaired volunteers put on the exoskeleton and adjusted the waist cuff, thigh cuffs, and sliders to their preference. All users reported the exoskeleton was comfortable, and there were no uncomfortable protrusions. Two users reported the small thigh cuffs were too small, a component that was able to be swapped out for a larger size. One participant reported discomfort from the motor assembly but said they would be able to wear it for several walking trials. The final comfort rating of the hip exoskeleton was 2.5 out of 3, satisfying the engineering requirement.

6.6 Protruding Distance

Arm swing is common during walking for efficiency and balance purposes. Due to this the hip exoskeleton must not interfere with the user's arm swing. A maximum exoskeleton protrusion distance of 4 cm at the hip is acceptable to have minimal interference with the user. The protrusion distance was measured at the maximum width of the exoskeleton leg which occurred at the shoulder bolt location of the pulley assembly. The protrusion distance was 3.75 cm, seen in Figure 21, satisfying the protrusion engineering requirement.

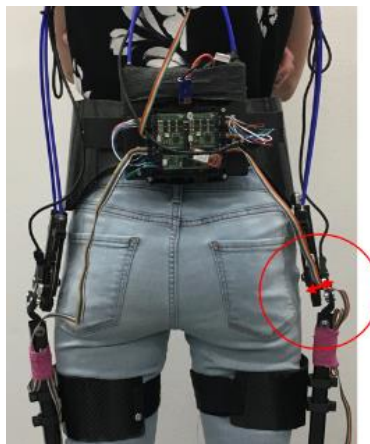


Figure 21: Hip exoskeleton protrusion distance

6.7 Range of Motion

To validate the hip exoskeleton range of motion, the device was placed in the maximum positions for abduction, adduction, flexion, and extension, and angle was measured with a digital protractor. The maximum flexion angle was 60.5° and maximum extension angle was 60° , totaling about 120° of total sagittal plane movement.

The two passive joints that allow user movement in the frontal plane included the pelvic hinge, and the hip joint hinge. The pelvic hinge has a maximum abduction angle of 40° , and a maximum adduction angle of 46° allowing the device to have a universal fit for different shaped users. The hip joint hinge which corresponds to the biological hip movement has a maximum abduction angle of 35° and maximum adduction angle of 36° .

The abduction, adduction, and extension movement requirements are satisfied; however, the hip exoskeletons flexion angle does not satisfy the 90° requirement for this design. The 90° angle requirement was to ensure a comfortable sitting position, however since 90° hip flexion is not required for walking, 60° maximum flexion will suffice for level ground walking for this version of the device.

7 Part A Conclusion

7.1 Summary

Part A of this thesis focused on introducing an ultra lightweight hip exoskeleton for research in the NAU Biomechatronics Lab. The final mechanical design was manufactured and validated per the engineering requirements stated in Table 2. The hip exoskeleton satisfied all engineering requirements with the exception of torque tracking for large torque applications, and flexural ROM for comfortable sitting.

The hip exoskeleton introduced in Part A was the lightest bilateral-bidirectional hip exoskeleton in the literature. The exoskeleton allowed sizing adjustments between users making it quick and easy for different users to use the device. The hip exoskeleton had a small protrusion distance and had the ability to apply large torques to the user, comfortably assisting with level ground walking.

7.2 Contributions

The development of the ultra-light weight powered hip exoskeleton was a collaborative effort. I designed and manufactured the mechanical system while PhD student Safoura Sadegh Pour Aji Bishe developed and tested the control system to operate the device. Together, we ensured the hip exoskeleton operated as required for validation purposes and for use in future studies.

7.3 Future Work

This hip exoskeleton design is the first of its kind in the NAU Biomechatronics Lab and will continually be redesigned and updated as required. A new version of the hip exoskeleton

will be developed to address the large cables located on the back, and flexion range of motion to allow comfortable use during stair climbing.

A new hip exoskeleton design will include a motor housing design allowing the Bowden cable to exit the motor housing from the side, similar to Prototype A, but will terminate at the hip joint horizontally, effectively removing large or sharp Bowden cable curvature and minimizing the design.

The control system for the hip exoskeleton will be continually updated until torque tracking reaches a minimal RMSE value of less than 1.2 Nm during large torque applications. This will require minimal noise in the system and will increase comfort for the user during torque application.

Part B: Passive Ankle-Foot Orthosis
(AFO) with Adjustable Assistance

8 Background

8.1 Ankle Kinematics

The ankle joint has 3-DOF: movement on the sagittal plane known as plantarflexion and dorsiflexion, movement on the frontal plane known as inversion and eversion, and movement on the transverse plane known as abduction and adduction. Plantar and dorsiflexion are the primary motions while walking where plantarflexion is the motion of pointing the toe away from the leg and dorsiflexion is the motion of pulling the toe towards the shank. For plantarflexion and dorsiflexion of the ankle, an unimpaired individual has about 40° ROM on the sagittal plane with 20° dorsiflexion and 20° plantarflexion shown in Figure 22 [31]. Inversion and eversion have smaller movements during walking. For an unimpaired individual, the angle of inversion is about 3° and eversion is 8° [35].

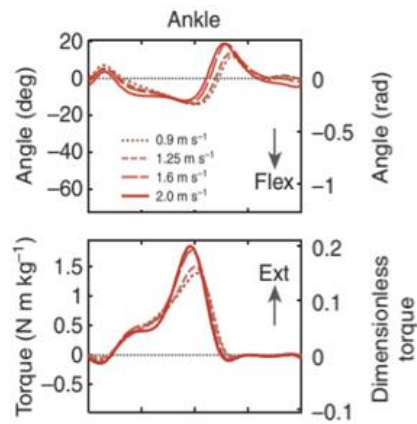


Figure 22: Ankle kinematics during differing walking speeds [31]

8.2 Ankle-Foot Orthoses (AFOs)

AFOs are common forms of biomechanical adjustment that add stiffness to the ankle joint to avoid unwanted misalignment while walking [10]. There are two different types of AFOs that can be used for different impairment levels: articulated, and non-articulated. Articulated AFOs are designed to combine lightweight materials and joints to create a hinged boot or flexion stops to control the ankle movement. Non-Articulated AFOs can range from rigid to flexible depending on the required use [10]. Rigid AFOs are used to hold the ankle in the flexed position and restrict all plantarflexion movement, however if an AFO is too rigid, it may cause excessive knee flexion hindering the user. The flexible types of AFOs allow more ankle movement and are less stable, these types of AFOs tend to focus on assisting with toe-off [10]. AFOs can be custom made to fit different users' needs such as fixing plantarflexion weakness or drop-foot, making them very common for treating CP patients [11]–[14].

Individuals with CP have lower ankle mobility when compared to their unimpaired counterparts. Decreasing ankle mobility further may keep their ankle in a natural position but does not allow the individuals to activate the muscles required for plantar and dorsiflexion [14].

8.3 Relevance to Field

Individuals with CP have reduced gait performance including excessive hip, knee, and ankle flexion, as well as ankle plantarflexion weakness [24]. These reduced gait performance issues can cause crouch gait, drop-foot, slower walking speeds, and smaller steps, making it more difficult to walk overall. AFOs are commonly prescribed for plantarflexion weakness or excessive plantarflexion to help correct crouch gait or drop-foot [11], [13]. A 2012 survey showed that about 85% of all CP patients use an orthotic device and 21.8% of all CP patients use

an AFO to help treat their condition [9]. Studies have shown that using an AFO can decrease MCoT for impaired individuals [60]–[63], indicating a promise for this technology in CP users.

The next section of this thesis will look into 3 types of AFO systems: solid ankle foot orthoses, posterior leaf spring AFOs, and pneumatic muscles. Each design in the literature will be evaluated to determine design successes and shortfalls. That information will then be used to discuss design parameters for the AFO in Chapter 10 and the design process in Chapter 0. Design validation will then be discussed in Chapter 0 to ensure the device meets the design parameters.

9 Literature Review

The following chapter discusses recent advancements in AFO designs. Each device was examined for specific mechanical features including stiffness, weight, ROM, and effectiveness. The following information was used to determine an optimal design for the adjustable AFO.

9.1 Solid Ankle-Foot Orthoses (SAFO)

Solid Ankle-Foot Orthoses are common types of AFOs used to treat a variety of movement impairments [14], [64]. SAFOs are stiff boot-like structures that encase the foot and lower leg to prevent ankle movement and are known to be the most restrictive, but most stable type of AFO [14]. SAFOs are typically made of thermoplastic to allow the device to be custom fit to the user. The goal of the SAFO is to completely restrict all movement of the ankle and help prevent issues such as drop-foot during everyday activities [14]. An example of the SAFO type is shown in Figure 23.



Figure 23: Solid Ankle-Foot Orthosis [14]

SAFOs can cause further issues in individuals by reducing the ankle ROM and therefore reducing the ankle power during toe-off making it more difficult to walk. These types of orthoses are common in correcting drop-foot during swing but lack other useful traits.

9.2 Posterior Leaf Spring Ankle-Foot Orthoses (PLS AFO)

PLS AFOs are becoming increasingly popular due to their ability to return energy during the gait cycle. Many PLS AFOs are made from carbon fiber leaf springs located behind the foot. These custom made AFOs allow for variable stiffnesses by modifying the lever arm of the leaf spring, or switching the leaf spring all together [61], [62], [65]–[67].

A carbon fiber posterior leaf spring AFO can be seen in Figure 24 [61]. All PLS AFOs include a calf brace made from a stiff material customized to the user, a customized stiff footplate and a leaf spring attached to the back of the calf and heel portion of the leg. When the user dorsiflexes during stance phase, the leaf spring deforms storing energy, and releases the energy back to the user during toe-off [66], [67]. A study quantifying effectiveness of PLS AFOs determined the carbon spring contributed 62% of the maximum total ankle power during push-off [67]. In order to effectively actuate the leaf spring, PLS AFOs are set with a neutral angle of 0° to 8° in the plantarflexion direction [62], [66], [68]. With a reduced ankle ROM – much like the SAFO devices – the ability to generate ankle power decreases [13], [69], indicating it is important to allow natural range of motion if the main goal is to increase ankle power during toe-off.

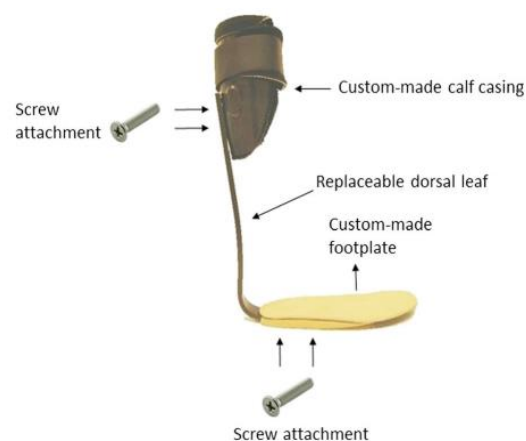


Figure 24: Posterior Carbon Fiber Leaf Spring AFO [61]

Several studies analyzed the effects of a flexible vs stiff PLS AFO on different patient populations, several of which determined there is an optimal leaf spring stiffness. If the AFO is too stiff, it reduces ankle dorsiflexion movement and negatively affects ankle power. If the AFO is too flexible, the user's gait kinematics remain unchanged, as if they were not using a device [60], [61], [65].

Carbon fiber PLS AFOs show promise relative to SAFOs due to the increased range of motion and increased ankle power during toe off. These devices are relatively lightweight, only comprising of a calf attachment and foot plate with a thin leaf spring connecting the two. However, these types of AFOs restrict movement in one direction depending on what they were made for – plantarflexion assistance or dorsiflexion assistance. PLS AFOs are not made to assist with both plantar and dorsiflexion.

9.3 Unpowered Exoskeleton

The unpowered ankle exoskeleton acts in the same way as many dynamic AFOs, storing energy in a spring during stance phase and releasing the energy back to the user during toe-off. Figure 25 shows the unpowered exoskeleton design with respect to the lower leg [60]. The design includes a mechanical clutch located directly behind the calf muscle to hold the tension spring which spans from the back of the heel to the upper calf muscle. The device is designed to work in parallel with the calf muscle by assisting plantarflexion during toe-off much like the Achilles tendon [60]. The spring engages when the foot is in contact with the ground and disengages when the foot is lifted through the use of a clutch, producing an ankle torque at toe off. The study looked at muscle activation and torque patterns for 9 healthy participants, concluding reduced calf muscle activation, similar torque profiles, and lower torque magnitudes while using the device when compared to unassisted walking [60].

Much like the previous PLS AFOs, this study concluded there is an optimal spring stiffness for each participant, estimating the average optimal stiffness to be about $175 \frac{\text{Nm}}{\text{rad}}$ for a participant weighing 77.4 kg. One leg of the unpowered exoskeleton has a total mass of 0.408 kg and 0.503 kg for a medium and large size respectively.

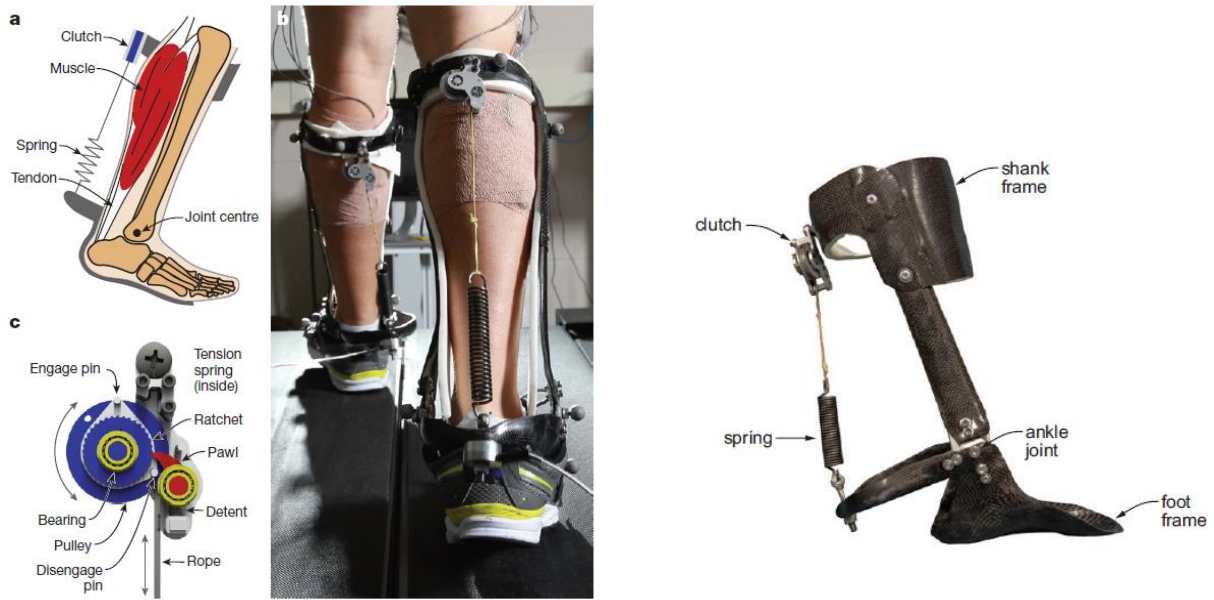


Figure 25: Passive Unpowered Ankle Exoskeleton [60]

This device showed promising results while testing on healthy participants. The device is relatively lightweight, has adjustable stiffness by swapping the leaf spring, and does not restrict ankle ROM. However, it has a large protrusion at the back of the heel which makes it difficult to go downstairs, complete everyday tasks, and does not assist with drop-foot during the swing phase.

9.4 Pneumatic Muscle Ankle Exoskeleton

Pneumatic muscle exoskeletons are known to produce high torques and act in a similar fashion as the unpowered exoskeleton by retracting lever arms attached from the shank to the

foot. One study looked at the effectiveness of one vs two pneumatic muscles in parallel [70]. The device can be seen in Figure 26. The total weight of the device is 1.3 kg and 1.7 kg for the single and double muscle devices respectively [70]. One pneumatic muscle could provide up to 57% of the maximum ankle plantarflexor torque during stance, showing promising results for ankle power during toe-off.



Figure 26: Artificial pneumatic muscle powered ankle exoskeleton. (a) single muscle, (b) dual parallel muscle [70]

Another similar device included bidirectional capabilities through the use of two artificial pneumatic muscles on the posterior and anterior side of the shank. The device can be seen in Figure 27. This device assists with both plantarflexion during toe-off and helps avoid drop-foot during swing. One leg of the bidirectional pneumatic muscle exoskeleton weighs 1.7 kg. The exoskeleton is EMG controlled using the soleus muscle for plantarflexion assistance and the tibialis anterior for dorsiflexion assistance. This ensures the torques will be applied at the appropriate time for the most beneficial assistance [71]. During subject testing, the device provided 50.7 Nm of plantarflexion torque and 20.7 Nm of dorsiflexion torque, equating to about 36% and 123% of the natural biological torques, respectively.

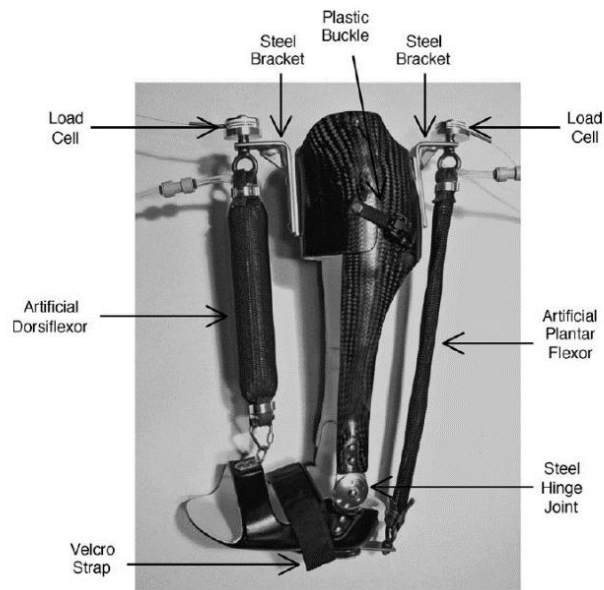


Figure 27: Dual artificial pneumatic muscle for dorsi and plantarflexion assistance [71]

The artificial pneumatic muscle exoskeletons can provide large amounts of torque by inflating the mesh tubing with compressed air to shorten the artificial muscle and provide a moment about the biological ankle through lever arms [70], [71]. However, this type of design is not universal due to the device bulkiness, and the necessity to be tethered to a compressed air tank to actuate the muscles. For this reason, the pneumatic muscles were not considered for a lightweight AFO design.

10 Design Criteria

The adjustable AFO was designed and validated to specific engineering requirements, outlined below. The AFO will be used to assist individuals with ankle joint correction while walking, including increasing ankle power during toe off, and assisting with drop-foot during swing. Specific design criteria for the AFO include weight, ROM, leaf spring stiffness, and user comfort comparable to devices in the literature.

10.1 Weight

The AFO will meet weight requirements of current AFOs represented in the literature. Minimizing AFO weight is important for AFO effectiveness and user comfort. The larger the device, the more difficult it is to walk efficiently, similar to attaching an ankle weight. The AFO will have a weight requirement of 0.4 kg for one leg, including the footplate and shank attachments.

10.2 Stiffness

The AFO must have adequate stiffness to assist the ankle during toe-off and must be able to return the foot to the neutral position during swing. The leaf spring stiffness will be quantified using beam bending equations and validated experimentally. The leaf spring stiffness will be compared to other leaf spring AFOs in the literature.

10.3 Fast AFO Modification

The device must be easily modified for different sized users and quick to put on and take off. The AFO must allow for quick stiffness modifications without switching the leaf spring, as well as fast shank and footplate replacements. This will allow the device to be more universal

between users. The time required to modify the AFO footplate, cuff, and stiffness will be under 2 minutes for an experienced user.

10.4 Range of Motion

During level ground walking, the AFO must not restrict a healthy individuals natural ankle angle. The AFO ankle angle will be measured using a benchtop test and compared to a healthy individuals ankle kinematics.

10.5 User Comfort

The AFO device will be comfortable for all users while walking. The user should comfortably be able to wear the device for a minimum of 30 minutes at a user specified stiffness. Three unimpaired volunteers will try on the device and adjust the stiffness level to their liking. The user will then walk around in the device to determine any areas of discomfort and rate the device comfort on a scale of 1 to 3, 1 being impossible to wear, 2 being comfortable to wear for 30 minutes, and 3 being extremely comfortable.

A summary of the engineering requirements for the AFO device are in Table 3.

Table 3: AFO Engineering Requirements

Requirements	Validation
Weight < 400 g for 1 leg	Weigh with scale
Quantify variable stiffness for 1/16", 1/8", and 3/16" leaf springs	Estimate stiffness of the device through composite beam bending, validate with experimentally by measuring beam stiffness
Ability to modify AFO: Change leaf spring stiffness, cuff, and footplate < 2 minutes	Time how long it takes for 1 person to change the leaf spring stiffness, replace the calf cuff, and replace the footplate for one device.
< 60 seconds to don or doff the device	Time how long it takes for 1 person to put on and take off one AFO device.
≥ biological ankle range of motion for level walking	Measure maximum and minimum range of motion of the device during benchtop testing.
Comfortable rating ≥ 2	Have 3-5 volunteers try on device and rate comfort from 1-3. 1 = impossible to wear 2 = some discomfort in spots, but can be worn for 30 minutes 3 = extremely comfortable.

11 Design Concepts

11.1 Prototype

The AFO prototype was designed to help assist individuals increase ankle power at toe off and return the foot to a neutral position to avoid drop-foot during swing for level ground walking. The prototype can be seen in Figure 28. It includes a square tube upright housing the leaf springs, pulley assembly, shin cuff, footplate, and upright slider. Three carbon fiber leaf springs – one 1/16” beam for dorsiflexion assistance, and two 1/8” beams for plantarflexion assistance – were used to assess the initial stiffness of the AFO during walking. The leaf spring stiffness could be adjusted by moving the upright slider up or down, effectively shortening or lengthening the beam for a rigid or flexible AFO.

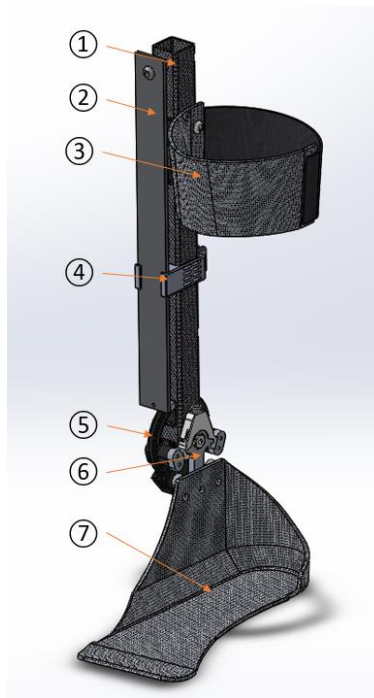


Figure 28: Prototype for AFO Device. (1) upright, (2) plantarflexion assist leaf spring, (3) shin cuff, (4) upright slider, (5) ankle pulley, (6) torque sensor, (7) footplate

The leaf springs were attached to the upper portion of the upright with a shoulder bolt and spacers, ensuring the leaf springs had 1 cm of deflection distance between the upright and neutral

position. Cables attached to the bottom of the leaf spring and were secured around the ankle pulley. When the pulley was rotated in either plantar or dorsiflexion directions, the respective leaf spring deflected storing power in the device until it was released to the user later in the gait cycle.

The prototype pulley assembly included the same 3D printed pulley for the hip exoskeleton. This allowed the AFO to use the same torque sensors during validation to assess assistance torque at different degrees of rotation.

To make the AFO customizable for different users, the footplate and shin cuff were replaceable. The footplate was fastened to the torque sensor with screws, and the shin cuff was attached to the upright with dual sliders seen in the final version of the hip exoskeleton.

During testing of this prototype, future improvements were noted:

- Pulley deformation during plantarflexion spring loading
- Uncomfortable shin cuff
- Carbon fiber upright cracked due to high torsion
- Unnecessary heavy components
- Excess movement before spring engagement
- Does not return foot to neutral position during swing

11.2 Final Design

The final AFO design included updates to the cuff, upright, and pulley assembly. The cuff was changed from a shin cuff to a calf cuff to help improve comfort during walking. The cuff has two sliders, the lower one keeping the cuff in line with the upright, and the upper one allowing height adjustability or cuff replacement. The final design can be seen in Figure 29.



Figure 29: Final AFO Design. (1) upright, (2) cuff sliders with tightening cam mechanisms, (3) calf cuff, (4) plantarflexion assist leaf spring, (5) dorsiflexion assist leaf spring, (6) upright slider with tightening cam mechanism, (7) ankle pulley, (8) pulley-to-footplate adapter, (9) footplate

The upright used in the prototype was a square tube from Rockwest composites with thin walls to minimize weight, however after upright failure occurred in the prototype the wall thickness of the square tube upright was increased.

To address pulley deformation, a custom pulley was designed with a stronger bridge than the previous version. Instead of relying on the pulley arc to disperse the force, a new pulley was designed with a screw bridging the two sides of the pulley, effectively stiffening the bonded connection between the two sides. The connection points to the existing torque sensor were modified as well, placing two bolts near the bridge of the pulley and two bolts near the footplate connection. These geometric modifications improved pulley durability, however with these modifications, the torque sensor no longer fit the system. The deformed pulley and proposed pulley design can be seen in Figure 30.

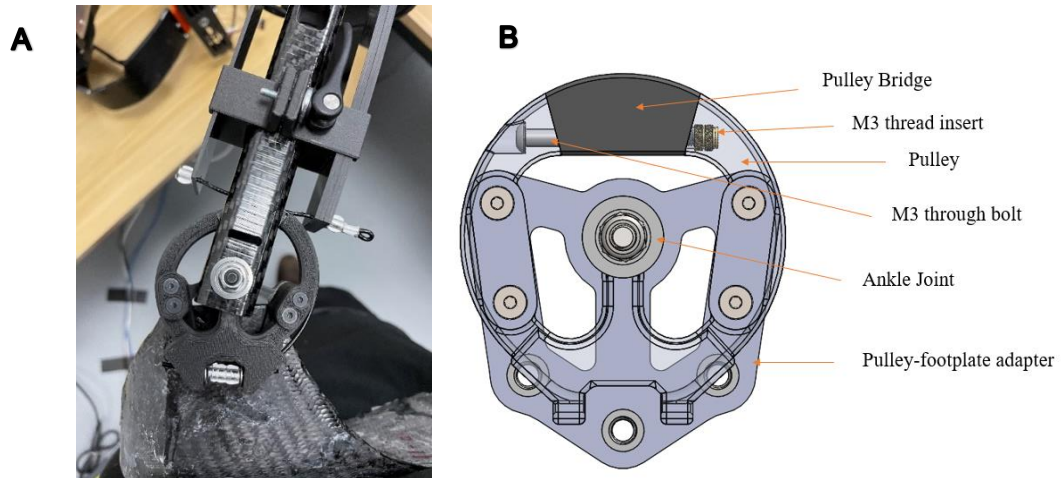


Figure 30: Reinforced Pulley Geometry. A) deformed prototype pulley, B) new proposed pulley design

To minimize weight of the system, several components were replaced. The two-bar leaf spring for plantarflexion assistance was replaced by one 3/16" carbon fiber bar. This allowed for similar stiffness while decreasing the weight of the leaf spring components. The 6 mm shoulder bolt connecting the leaf spring to the upright was replaced with a 4 mm shoulder bolt. The aluminum torque sensor attached to the pulley was not compatible with the new pulley design, so the new pulley-to-footplate adapter replacing the torque sensor was 3D printed from onyx and carbon fiber.

The excess movement in the system before the spring engaged was fixed by repositioning the neutral angle of the device. The neutral angle, like many AFO's discussed in the literature, was set to about 8° in plantarflexion. When the cables were placed, they were drawn taught before crimping to ensure the movement in the system was minimized.

12 Design Validation

To validate the AFO mechanical design, engineering requirements from Table 3 were tested. Six engineering requirements were validated: weight, quantifying stiffness, ability to change stiffness, ease to don and doff device, natural ankle angle interference, and comfortability.

12.1 Weight

The minimal AFO without the footplate or cuff weighed 202g. This included the pulley assembly, upright, upright slider, and two leaf springs – 1/8” and 3/16” carbon fiber bars. The weight is variable depending on leaf spring preference. For validation purposes, I choose to use the two larger leaf springs for the worst-case scenario. Depending on the size of the user, the weight can range from 350g to 450g. For a small user with a men’s shoe size 5, the total weight of one AFO is 372g. For a large user with a men’s shoe size 13, the total weight of one AFO is 449g.

The AFO device meets weight requirements for the smaller version of the AFO, however it is above 400 g for the larger version. Comparing the larger AFO with other devices, 450 g weight is acceptable, meeting but not surpassing other designs of similar size [60].

12.2 Quantify Stiffness

Three leaf spring thicknesses were evaluated at varying lengths to determine the range of stiffness for different versions of the AFO. AFO stiffnesses were evaluated by determining the torque-angle relationship [60], [62] for the ankle joint, calculating torque per radian rotation. Each leaf spring – 1/16”, 1/8”, and 3/16” – was theoretically evaluated using composite beam bending, then placed in a testing jig to experimentally calculate the spring stiffness.

To calculate the theoretical stiffness of each carbon fiber beam, the cantilever beam bending equation was used. Equation 1 represents the estimated force, P, in kN required to deflect the beam a prescribed distance in mm, δ_{\max} , L is the length of the leaf spring in mm, E_f is the effective modulus of the carbon fiber beam in GPa, and I is the moment of inertia in mm^4 .

$$P = \frac{3 \delta_{\max} E_f I}{L^3} \quad (1)$$

The moment of inertia for a solid rectangular beam was calculated using Equation 2, where b was the width of the beam, and h was the thickness in mm.

$$I = \frac{b h^3}{12} \quad (2)$$

The effective modulus was estimated assuming the carbon fiber layup of each beam provided by Kinetic Composites Inc. For the small beam, 1/16", a layup of 9 layers was assumed with a layup orientation of [0/90 twill, [90, 0]₃, 90, 0/90 twill]. The medium beam, 1/8", was assumed to have 15 layers with a layup orientation of [0/90 twill, [90, 0]₆, 90, 0/90 twill]. The large beam, 3/16", was assumed to have 25 layers with a layup orientation of [0/90 twill, [90, 0]₁₁, 90, 0/90 twill]. Using the assumed layups, the effective modulus, E_f , for each beam was calculated using Equation 3, where h was the thickness of the laminate, E_x was the modulus of elasticity in the longitudinal direction for the j^{th} lamina, and z was the distance from the neutral axis to the top of the respective j^{th} lamina.

$$E_f = \frac{8}{h^3} \sum_{j=1}^{N/2} (E_x)_j (z_j^3 - z_{j-1}^3) \quad (3)$$

Once the effective modulus was calculated for each beam, it was then used in, Equation 1 for 40 different lengths along the beam to measure the required force to deflect each beam 1 cm. The stiffness of each beam at 40 different lengths was calculated in $\frac{\text{N}}{\text{mm}}$ using Equation 4, where P was the required force in N calculated from Equation 1, to deflect the beam 10 mm, δ .

$$k = \frac{P}{\delta} \quad (4)$$

The calculated stiffness in $\frac{N}{mm}$ was converted to $\frac{N}{rad}$ using Equation 5, where s was the linear travel distance, 10 mm, and r was the pulley radius, 30 mm. For 10 mm of beam deflection, the pulley had 10 mm of linear travel, resulting in 0.33 radians of rotation.

$$s = r\theta \quad (5)$$

Using 10 mm linear travel per 0.33 radians of rotation, a new stiffness value was given in $\frac{N}{rad}$. To determine the leaf spring stiffness in torque per radian $\left[\frac{Nm}{rad}\right]$ the previous stiffness value was multiplied by the pulley radius in meters, 0.03 m. The resulting theoretical data for leaf spring lengths ranging from 2 to 22 cm for the three leaf springs can be seen in Figure 31. For all three leaf springs, a power trendline was fit.

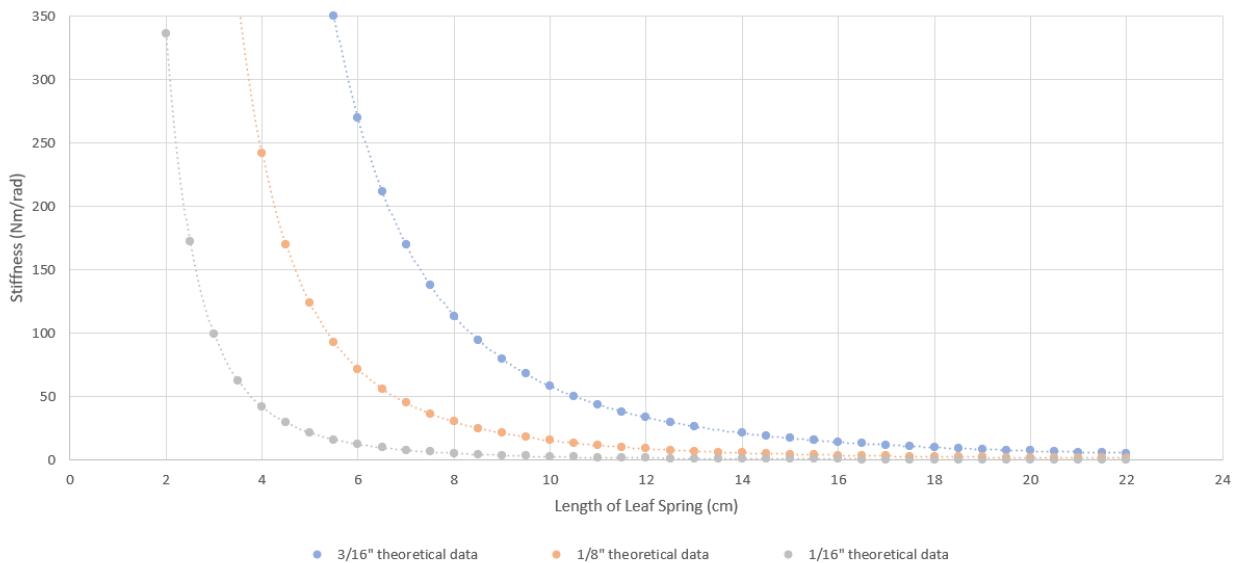


Figure 31: Theoretical stiffness for 3 thickness of leaf springs

To test the stiffness of each spring experimentally, a testing jig was set up to bend the beam a set distance and measure the force for the corresponding deflection. The testing jig can be seen in Figure 32 where the carbon fiber beam was bolted to a rail allowing the carbon fiber

bar to slide to different length positions. An aluminum bar with a piece of foam adhered to the end was bolted to the opposite side of the rail. The foam was measured, cut, and placed to ensure the carbon fiber beam would bend until just barely touching the tip of the foam, indicating a displacement of 1 cm. Foam was used as a stopper to ensure the measured force did not include a reaction force from the stopper. Force was measured using a Futek load cell attached directly to the carbon fiber beam using the same cable and stopper shown on the AFO. This ensured similar system behavior as the AFO.

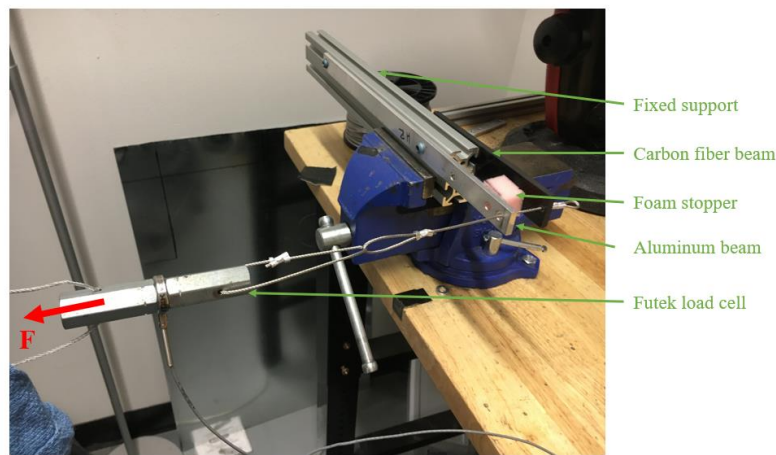


Figure 32: Beam stiffness testing jig

For the three carbon fiber bars, a variety of lengths were assessed, measuring the force required to deflect the beam 1 cm. Ten data points were collected at varying lengths for the 1/16” and 1/8” beams, but due to stiffness limitations only eight data points were collected for the 3/16” beam. The load data was collected through the ankle exoskeleton GUI, and post processed.

The leaf spring stiffness, k in $\frac{N}{mm}$, was determined using Equation 4, where the force was measured in Newtons.

Once the spring stiffness was determined for each location along the beam, a stiffness per radian of pulley rotation was determined by Equation 5. The pulley used for the AFO has a radius of 30 mm. For 10 mm of leaf spring deflection, the pulley would rotate 0.333 radians. The spring stiffness value, k , was then converted from $\frac{N}{mm}$ to $\frac{N}{rad}$.

Torque per radian rotation was determined by multiplying beam stiffness in Newtons per radian by the pulley radius in meters to determine spring stiffness in $\frac{Nm}{rad}$. The results of the three leaf springs can be seen in Figure 33.

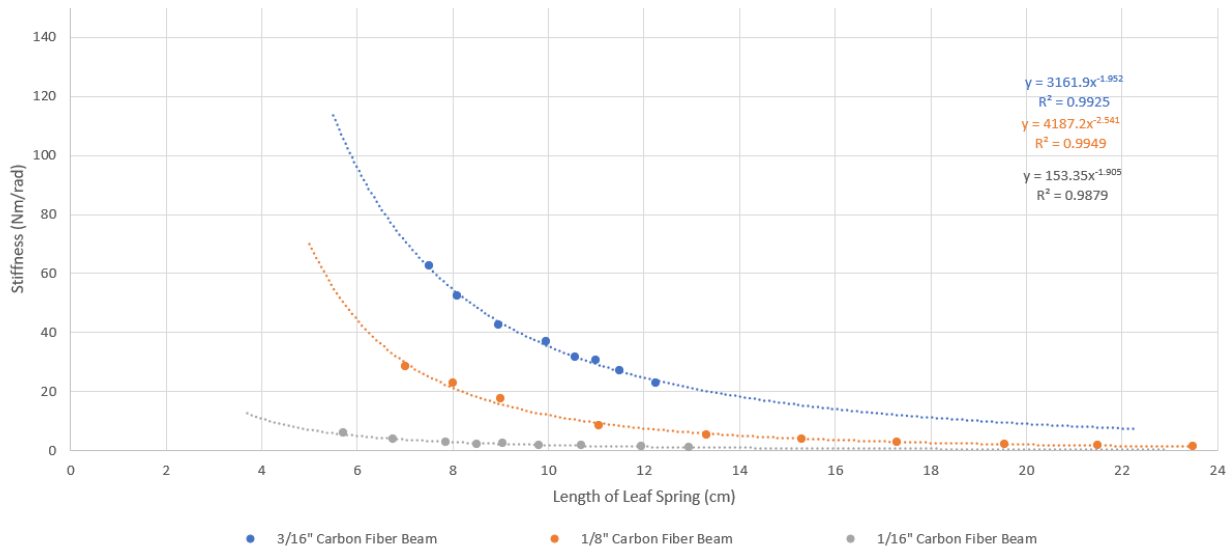


Figure 33: Three thickness leaf springs evaluated at different lengths to determine torque per rotation relationship for AFO stiffness evaluation

After data collection was complete, the theoretical data was compared to the experimental data to determine accuracy of the results. The results for the theoretical vs experimental data can be seen in Figure 34.

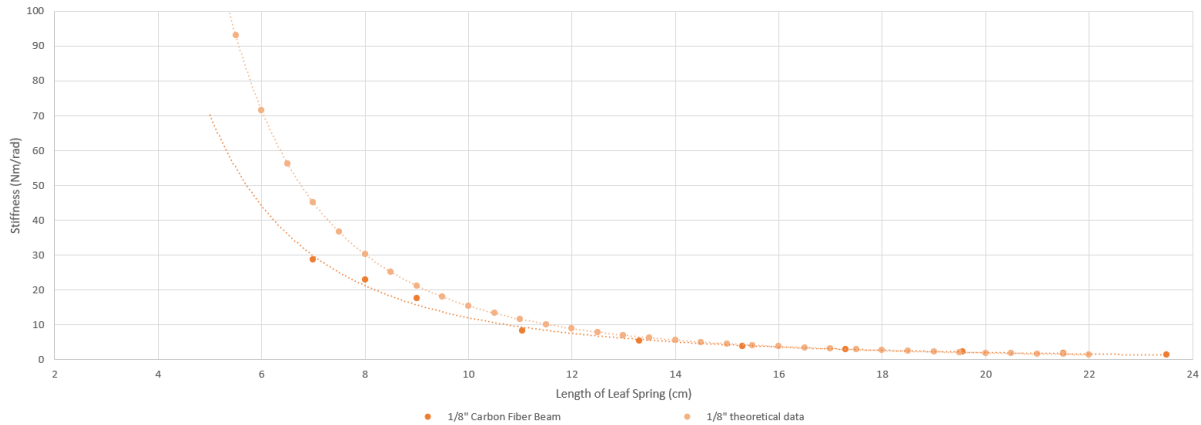


Figure 34: Theoretical and experimental data for 1/8" leaf spring

The experimental results do not match the theoretical results in magnitude for shorter lengths, but they resemble a similar power curve for the 1/8" beam. The experimental and theoretical results were expected to differ due to the unknown material properties of the composite beam. The carbon fiber bars provided from Kinetic Composites gave a layer range for each bar, specified the basic layer orientations, and did not provide the type of carbon fiber or resin system used. The number of layers for each bar was estimated at 6-9, 14-16, and 24-26 layers for the 1/16", 1/8", and 3/16" beams, respectively. The layup orientation for each bar was specified as a simple weave for the outer plies and alternating 0° and 90° unidirectional plies between the outer layers. Because the carbon fiber and resin systems were not specified, the longitudinal and transverse moduli were estimated based on intermediate modulus carbon fiber systems obtained from Rockwest composites. Due to the unknown composite properties, assumptions about the layer sequence, number of layers, and material properties were made to calculate the theoretical bending stiffness, resulting in a larger uncertainty. To improve the theoretical data for each beam, specific composites properties would be required. To improve the experimental data for all three beams, additional data would be required for different lengths, and a more accurate deflection measuring tool would be necessary to increase accuracy of the test.

For the 1/16” and 3/16” beams specifically, additional data for longer length beams would be required to accurately estimate the experimental stiffness curve.

The Sawicki passive exoskeleton reported an optimal stiffness of $175 \frac{\text{Nm}}{\text{rad}}$ [60], and another spring-like AFO reported an average of $364.4 \frac{\text{Nm}}{\text{rad}}$ [62]. The proposed AFO design has varying leaf spring lengths between 2 and 12 cm, but additional high force testing between lengths of 2 and 5 cm is required to determine if the AFO can meet stiffness requirements of other published devices.

12.3 Fast AFO Modification

Fast AFO modifications were evaluated by determining the minimum time it took to change the leaf spring length, replace the calf cuff, and replace the footplate. The total time to change the three components had to be under 2 minutes for an experienced user.

The leaf spring stiffness took about 11 seconds to change the slider from top (most flexible) to bottom (stiffest), and about 10 seconds to move the slider from the bottom to the top.

To change the calf cuff, one of the two sliders included a camming mechanism that when unfastened, allowed free movement of the cuff along the upright. It took about 6 seconds to unfasten and separate the cuff from the upright, and about 22 seconds to put the cuff on the upright.

Footplate modification included unfastening 3-M5 screws attaching the footplate to the adapter and reattaching the same 3 screws to a new footplate. Using a hand-held screwdriver to unfasten the bolts, it took about 33 seconds to take off the footplate, and about 52 seconds to put a new footplate on the device.

In total, it took about 1 minute and 50 seconds to replace a calf cuff and footplate on one side of the AFO device. If the leaf spring needed to be adjusted, the time required to modify one AFO device would be approximately two minutes, satisfying the quick modification engineering requirement.

12.4 Time to don and doff AFO

Five trials of donning and doffing the AFO device were evaluated to determine ease of use. The user started with a pair of shoes and the AFO device separated. The user then put the footplate of the AFO device under the insole of the shoe, stepped into the shoe, tied the shoe, and attached the cuff around their shank and started walking. The average time of the five trials was about 34 seconds to put on the device, and about 14 seconds to take off the device, satisfying the time constraint of don/doff in less than one minute.

12.5 Natural Ankle Angle Interference

To evaluate if the AFO interfered with ankle movement during walking, a benchtop test was conducted. The benchtop test measured the maximum deflection angle for both dorsi and plantarflexion. The maximum dorsiflexion angle was measured at 25.3° and maximum plantarflexion angle measured at 37.8° adding to a total of 63.1° ankle rotation. A healthy individual walking on level ground has about 40° sagittal plane movement mentioned previous. Comparing the benchtop results to a healthy individuals ankle ROM during walking, the device satisfies ROM requirements.

12.6 Comfort

Three unimpaired volunteers rated the comfort of the AFO. All participants changed the stiffness to find a comfortable assistance level and walked on level ground for several minutes.

All participants reported the AFO was comfortable to wear and did not impede their normal walking patterns while using the lowest stiffness settings. Some users reported discomfort during high stiffness walking from excess rotation of the device around their leg. Since many users adjusted stiffness based on their own comfort feedback, a comfort rating of 3 out of 3 was achieved for this device. The proposed AFO device satisfies the comfort requirements and was able to be worn for at least 30 minutes without any discomfort at a user specified stiffness.

13 Part B Conclusion

13.1 Summary

The primary goal of this thesis was to design and validate the mechanical design of a dual leaf spring AFO for use in clinical research settings within the NAU Biomechatronics Lab. The AFO device was prototyped and redesigned to ensure optimal performance. The device was then validated for stiffness, weight, comfort, and performance. The AFO device met requirements for stiffness, comfort, performance, and weight requirements for a small version, however it did not meet weight requirements for a large version of the device.

The AFO introduced in Part B was the only quick adjustable AFO in the literature. The AFO allowed sizing adjustments between users by modifying the shank and footplate attachments. The stiffness was easily modified by sliding a mechanism along the length of a carbon fiber leaf spring to effectively changing the AFO stiffness in a matter of seconds.

13.2 Future Work

Device validation and successful market products researched for this thesis prompted future design ideas for this device. Many market and research AFOs allow for neutral angle adjustment. The proposed design has a permanent neutral ankle of about 8° plantarflexion, which can be helpful for some users, but detrimental to others depending on impairment level and type. A future version of this AFO design will include a tuning mechanism seen on any string instrument to precisely adjust the neutral angle of the ankle position to allow more customized modifications for the user.

Currently the leaf springs are located on the outside of the tube, creating pinch points for users. A newer version will investigate putting the leaf springs inside a larger rectangular tube, encasing the entire system providing protection to the device and the user.

The presented design allows both the dorsi and plantarflexion leaf springs to be adjusted together, but there is currently no way to adjust only one stiffness without the other. An updated AFO design will include independent adjustability for both the dorsiflexion and the plantarflexion leaf springs allowing the device to be more customizable to the user's specific needs.

Finally, the device torque should be verified in future studies with an instrumented torque sensor at the ankle. This would only be used for verification purposes of future designs to determine the torque per radian rotation relationship. Once torque relationships are determined for different leaf spring lengths, users could accurately determine their optimal stiffness for different activities such as running or walking.

14 Conclusion

Cerebral Palsy is the most common form of disability in children, affecting movement and muscle activation [3]–[6]. Treatments for CP such as surgery, physical therapy, orthotic devices, and locomotion training, have shown varying promise [9]–[14]. Studies on accessible orthotic devices have shown improved mobility in individuals with CP due to increased ankle stabilization. However, AFOs are typically extremely rigid and can negatively affect ankle power. Similarly, exoskeleton enhanced locomotion training has been shown to improve gait patterns, but all CP specific studies focus on knee extension or ankle assistance and hip exoskeleton studies utilize designs too heavy to be viable in assisting children [15]–[18].

In Part A of this thesis, I introduced an ultra-lightweight bilateral hip exoskeleton designed for assisting individuals with CP. The device was the lightest bilateral hip exoskeleton in the literature, ensuring the MCoT while using the device was minimized. The hip exoskeleton successfully applied an assistive hip torque of 12 Nm while securely fitting different sized users. The development of this device will give the NAU Biomechatronics Lab the potential to conduct research on hip assistance for children with CP.

Part B of this thesis introduced an adjustable AFO device designed for assisting individuals with plantarflexor weakness and drop-foot. This device was designed to allow natural ankle ROM, provide plantarflexion assistance, and have quickly adjustable stiffness to account for different user and situational needs. This was the only quickly adjustable AFO device in the literature that did not require replacing a leaf spring to adjust stiffness levels.

The ultra-lightweight hip exoskeleton and adjustable ankle-foot orthosis devices bring us one step further in improving patient mobility.

References

- [1] M. L. Aisen *et al.*, “Cerebral palsy: Clinical care and neurological rehabilitation,” *The Lancet Neurology*. 2011, doi: 10.1016/S1474-4422(11)70176-4.
- [2] R. L. Waters and S. Mulroy, “The energy expenditure of normal and pathologic gait,” *Gait and Posture*. 1999, doi: 10.1016/S0966-6362(99)00009-0.
- [3] P. Rosenbaum, N. Paneth, A. Leviton, M. Goldstein, and M. Bax, “A report: The definition and classification of cerebral palsy April 2006,” *Developmental Medicine and Child Neurology*. 2007, doi: 10.1111/j.1469-8749.2007.tb12610.x.
- [4] M. Bax *et al.*, “Proposed definition and classification of cerebral palsy, April 2005,” *Developmental Medicine and Child Neurology*. 2005, doi: 10.1017/S001216220500112X.
- [5] M. C. Macintosh, “CEREBRAL PALSIES: EPIDEMIOLOGY AND CAUSAL PATHWAYS,” *Obstet. Gynaecol.*, 2001, doi: 10.1576/toag.2001.3.1.48.1.
- [6] C. Bayon and R. Raya, “Robotic Therapies for Children with Cerebral Palsy: A Systematic Review,” *Transl. Biomed.*, 2016, doi: 10.21767/2172-0479.100044.
- [7] J. Rose, J. G. Gamble, A. Burgos, J. Medeiros, and W. L. Haskell, “ENERGY EXPENDITURE INDEX OF WALKING FOR NORMAL CHILDREN AND FOR CHILDREN WITH CEREBRAL PALSY,” *Dev. Med. Child Neurol.*, 1990, doi: 10.1111/j.1469-8749.1990.tb16945.x.
- [8] D. B. Maltais, M. R. Pierrynowski, V. A. Galea, and O. Bar-Or, “Physical activity level is associated with the O₂ cost of walking in cerebral palsy,” *Med. Sci. Sports Exerc.*, 2005, doi: 10.1249/01.MSS.0000155437.45937.82.
- [9] E. Sacaze *et al.*, “A survey of medical and paramedical involvement in children with cerebral palsy in Brittany: Preliminary results,” *Ann. Phys. Rehabil. Med.*, 2013, doi: 10.1016/j.rehab.2012.11.003.
- [10] M. Alam, I. A. Choudhury, and A. Bin Mamat, “Mechanism and design analysis of articulated ankle foot orthoses for drop-foot,” *Scientific World Journal*. 2014, doi: 10.1155/2014/867869.
- [11] Y. L. Kerkum, M. A. Brehm, A. I. Buizer, J. C. Van Den Noort, J. G. Becher, and J. Harlaar, “Defining the mechanical properties of a spring-hinged ankle foot orthosis to assess its potential use in children with spastic cerebral palsy,” *J. Appl. Biomech.*, 2014, doi: 10.1123/jab.2014-0046.
- [12] D. Maltais, O. Bar-Or, V. Galea, and M. Pierrynowski, “Use of orthoses lowers the O₂ cost of walking in children with spastic cerebral palsy,” *Med. Sci. Sports Exerc.*, 2001, doi: 10.1097/00005768-200102000-00023.
- [13] Y. L. Kerkum, A. I. Buizer, J. C. Van Den Noort, J. G. Becher, J. Harlaar, and M. A. Brehm, “The effects of varying ankle foot orthosis stiffness on gait in children with spastic cerebral palsy who walk with excessive knee flexion,” *PLoS One*, 2015, doi: 10.1371/journal.pone.0142878.
- [14] C. E. Buckon, S. S. Thomas, S. Jakobson-Huston, M. Moor, M. Sussman, and M. Aiona, “Comparison of three ankle-foot orthosis configurations for children with spastic diplegia,” *Dev. Med. Child Neurol.*, 2004, doi: 10.1017/S0012162204001008.
- [15] N. Smania *et al.*, “Improved gait after repetitive locomotor training in children with cerebral palsy,” *Am. J. Phys. Med. Rehabil.*, 2011, doi: 10.1097/PHM.0b013e318201741e.
- [16] M. Matsuda *et al.*, “Immediate effects of a single session of robot-assisted gait training using Hybrid Assistive Limb (HAL) for cerebral palsy,” *J. Phys. Ther. Sci.*, 2018, doi:

- 10.1589/jpts.30.207.
- [17] J. L. Pons, “Rehabilitation exoskeletal robotics. The promise of an emerging field.,” *IEEE Eng. Med. Biol. Mag.*, 2010, doi: 10.1109/MEMB.2010.936548.
- [18] T. M. O’Shea, “Diagnosis, treatment, and prevention of cerebral palsy,” *Clin. Obstet. Gynecol.*, 2008, doi: 10.1097/GRF.0b013e3181870ba7.
- [19] Z. F. Lerner *et al.*, “An Untethered Ankle Exoskeleton Improves Walking Economy in a Pilot Study of Individuals With Cerebral Palsy,” *IEEE Trans. Neural Syst. Rehabil. Eng.*, vol. 26, no. 10, pp. 1985–1993, Oct. 2018, doi: 10.1109/TNSRE.2018.2870756.
- [20] C. Buesing *et al.*, “Effects of a wearable exoskeleton stride management assist system (SMA®) on spatiotemporal gait characteristics in individuals after stroke: A randomized controlled trial,” *J. Neuroeng. Rehabil.*, 2015, doi: 10.1186/s12984-015-0062-0.
- [21] A. T. Asbeck, K. Schmidt, and C. J. Walsh, “Soft exosuit for hip assistance,” 2015, doi: 10.1016/j.robot.2014.09.025.
- [22] Y. Lee *et al.*, “A flexible exoskeleton for hip assistance,” 2017, doi: 10.1109/IROS.2017.8202275.
- [23] O. Bar-Or, O. Inbar, and R. Spira, “Physiological effects of a sports rehabilitation program on cerebral palsied and post-poliomyelitic adolescents,” *Med. Sci. Sports Exerc.*, 1976, doi: 10.1249/00005768-197600830-00004.
- [24] D. C. Johnson, D. L. Damiano, and M. F. Abel, “The evolution of gait in childhood and adolescent cerebral palsy,” *J. Pediatr. Orthop.*, 1997, doi: 10.1097/01241398-199705000-00022.
- [25] G. Orekhov, Y. Fang, J. Luque, and Z. F. Lerner, “Ankle Exoskeleton Assistance Can Improve Over-Ground Walking Economy in Individuals with Cerebral Palsy,” *IEEE Trans. Neural Syst. Rehabil. Eng.*, 2020, doi: 10.1109/TNSRE.2020.2965029.
- [26] Z. F. Lerner, D. L. Damiano, H. S. Park, A. J. Gravunder, and T. C. Bulea, “A Robotic Exoskeleton for Treatment of Crouch Gait in Children with Cerebral Palsy: Design and Initial Application,” *IEEE Trans. Neural Syst. Rehabil. Eng.*, 2017, doi: 10.1109/TNSRE.2016.2595501.
- [27] R. M. Andrade, S. Sapienza, and P. Bonato, “Development of a ‘transparent operation mode’ for a lower-limb exoskeleton designed for children with cerebral palsy,” 2019, doi: 10.1109/ICORR.2019.8779432.
- [28] D. Knudson, *The Fundamentals of Biomechanics - Second edition*. 2007.
- [29] D. Aaron and H. Hugh, “Lower Extremity Exoskeletons and Active Orthoses: Challenges and State-of-the-Art,” *IEEE Trans. Robot.*, 2008.
- [30] P. DeVita and T. Hortobagyi, “Age causes a redistribution of joint torques and powers during gait,” *J. Appl. Physiol.*, 2000, doi: 10.1152/jappl.2000.88.5.1804.
- [31] K. E. Zelik and A. D. Kuo, “Human walking isn’t all hard work: Evidence of soft tissue contributions to energy dissipation and return,” *J. Exp. Biol.*, 2010, doi: 10.1242/jeb.044297.
- [32] A. J. Young, H. Gannon, and D. P. Ferris, “A Biomechanical Comparison of Proportional Electromyography Control to Biological Torque Control Using a Powered Hip Exoskeleton,” *Front. Bioeng. Biotechnol.*, 2017, doi: 10.3389/fbioe.2017.00037.
- [33] H. K. Ramakrishnan and M. P. Kadaba, “On the estimation of joint kinematics during gait,” *J. Biomech.*, 1991, doi: 10.1016/0021-9290(91)90175-M.
- [34] C. L. Lewis and D. P. Ferris, “Invariant hip moment pattern while walking with a robotic hip exoskeleton,” *J. Biomech.*, 2011, doi: 10.1016/j.jbiomech.2011.01.030.

- [35] A. Phinyomark, S. T. Osis, B. A. Hettinga, D. Kobsar, and R. Ferber, "Gender differences in gait kinematics for patients with knee osteoarthritis," *BMC Musculoskelet. Disord.*, 2016, doi: 10.1186/s12891-016-1013-z.
- [36] A. M. Dollar and H. Herr, "Lower extremity exoskeletons and active orthoses: Challenges and state-of-the-art," *IEEE Trans. Robot.*, 2008, doi: 10.1109/TRO.2008.915453.
- [37] D. Paul and H. Tibor, "Age causes a redistribution of joint torques and powers during gait," *J. Appl. Physiol.*, 2000.
- [38] M. Q. Liu, F. C. Anderson, M. H. Schwartz, and S. L. Delp, "Muscle contributions to support and progression over a range of walking speeds," *J. Biomech.*, 2008, doi: 10.1016/j.jbiomech.2008.07.031.
- [39] K. Seo, J. Lee, Y. Lee, T. Ha, and Y. Shim, "Fully autonomous hip exoskeleton saves metabolic cost of walking," 2016, doi: 10.1109/ICRA.2016.7487663.
- [40] C. L. Vaughan, "Are joint torques the Holy Grail of human gait analysis?," *Hum. Mov. Sci.*, 1996, doi: 10.1016/0167-9457(96)00009-7.
- [41] Z. F. Lerner, D. L. Damiano, and T. C. Bulea, "The effects of exoskeleton assisted knee extension on lower-extremity gait kinematics, kinetics, and muscle activity in children with cerebral palsy," *Sci. Rep.*, 2017, doi: 10.1038/s41598-017-13554-2.
- [42] T. Lenzi, M. C. Carrozza, and S. K. Agrawal, "Powered hip exoskeletons can reduce the user's hip and ankle muscle activations during walking," *IEEE Trans. Neural Syst. Rehabil. Eng.*, 2013, doi: 10.1109/TNSRE.2013.2248749.
- [43] F. Giovacchini *et al.*, "A light-weight active orthosis for hip movement assistance," 2015, doi: 10.1016/j.robot.2014.08.015.
- [44] S. K. Banala, S. H. Kim, S. K. Agrawal, and J. P. Scholz, "Robot assisted gait training with active leg exoskeleton (ALEX)," 2009, doi: 10.1109/TNSRE.2008.2008280.
- [45] R. J. Farris, H. A. Quintero, and M. Goldfarb, "Preliminary evaluation of a powered lower limb orthosis to aid walking in paraplegic individuals," *IEEE Trans. Neural Syst. Rehabil. Eng.*, 2011, doi: 10.1109/TNSRE.2011.2163083.
- [46] H. Shimada *et al.*, "Effects of an automated stride assistance system on walking parameters and muscular glucose metabolism in elderly adults," *Br. J. Sports Med.*, 2008, doi: 10.1136/bjism.2007.039453.
- [47] Q. Wu, X. Wang, F. Du, and X. Zhang, "Design and control of a powered hip exoskeleton for walking assistance," *Int. J. Adv. Robot. Syst.*, 2015, doi: 10.5772/59757.
- [48] K. Junius, N. Lefeber, E. Swinnen, B. Vanderborght, and D. Lefeber, "Metabolic effects induced by a kinematically compatible hip exoskeleton during STS," *IEEE Trans. Biomed. Eng.*, 2018, doi: 10.1109/TBME.2017.2754922.
- [49] Y. Ding *et al.*, "Biomechanical and physiological evaluation of multi-joint assistance with soft exosuits," *IEEE Trans. Neural Syst. Rehabil. Eng.*, 2017, doi: 10.1109/TNSRE.2016.2523250.
- [50] A. T. Asbeck, S. M. M. De Rossi, I. Galiana, Y. Ding, and C. J. Walsh, "Stronger, smarter, softer: Next-generation wearable robots," *IEEE Robot. Autom. Mag.*, 2014, doi: 10.1109/MRA.2014.2360283.
- [51] S. H. *et al.*, "Effects of an automated stride assistance system on walking parameters and muscular glucose metabolism in elderly adults," *Br. J. Sports Med.*, 2008.
- [52] H. Shimada *et al.*, "Effects of a robotic walking exercise on walking performance in community-dwelling elderly adults," *Geriatr. Gerontol. Int.*, 2009, doi: 10.1111/j.1447-0594.2009.00546.x.

- [53] R. Kitatani, K. Ohata, H. Takahashi, S. Shibuta, Y. Hashiguchi, and N. Yamakami, "Reduction in energy expenditure during walking using an automated stride assistance device in healthy young adults," *Arch. Phys. Med. Rehabil.*, 2014, doi: 10.1016/j.apmr.2014.07.008.
- [54] A. Zoss, H. Kazerooni, and A. Chu, "On the mechanical design of the Berkeley Lower Extremity Exoskeleton (BLEEX)," 2005, doi: 10.1109/IROS.2005.1545453.
- [55] A. B. Zoss, H. Kazerooni, and A. Chu, "Biomechanical design of the Berkeley Lower Extremity Exoskeleton (BLEEX)," *IEEE/ASME Trans. Mechatronics*, 2006, doi: 10.1109/TMECH.2006.871087.
- [56] J. Babers, "Optimizing the Mechanical Design of an Untethered Ankle Exoskeleton," Northern Arizona University, 2020.
- [57] M. K. Ishmael, M. Tran, and T. Lenzi, "ExoProsthetics: Assisting above-knee amputees with a lightweight powered hip exoskeleton," 2019, doi: 10.1109/ICORR.2019.8779412.
- [58] D. Chen, Y. Yun, and A. D. Deshpande, "Experimental characterization of Bowden cable friction," 2014, doi: 10.1109/ICRA.2014.6907732.
- [59] N. Zakaria, "Children and teenagers body sizes and shapes analyses," in *Clothing for Children and Teenagers*, 2016.
- [60] S. H. Collins, M. Bruce Wiggin, and G. S. Sawicki, "Reducing the energy cost of human walking using an unpowered exoskeleton," *Nature*, 2015, doi: 10.1038/nature14288.
- [61] N. F. J. Waterval, F. Nollet, J. Harlaar, and M. A. Brehm, "Modifying ankle foot orthosis stiffness in patients with calf muscle weakness: Gait responses on group and individual level," *J. Neuroeng. Rehabil.*, 2019, doi: 10.1186/s12984-019-0600-2.
- [62] D. J. J. Bregman, J. Harlaar, C. G. M. Meskers, and V. de Groot, "Spring-like Ankle Foot Orthoses reduce the energy cost of walking by taking over ankle work," *Gait Posture*, 2012, doi: 10.1016/j.gaitpost.2011.08.026.
- [63] D. J. J. Bregman, V. De Groot, P. Van Diggele, H. Meulman, H. Houdijk, and J. Harlaar, "Polypropylene ankle foot orthoses to overcome drop-foot gait in central neurological patients: A mechanical and functional evaluation," *Prosthet. Orthot. Int.*, 2010, doi: 10.3109/03093646.2010.495969.
- [64] K. Desloovere *et al.*, "How can push-off be preserved during use of an ankle foot orthosis in children with hemiplegia? A prospective controlled study," *Gait Posture*, 2006, doi: 10.1016/j.gaitpost.2006.08.003.
- [65] E. Russell Esposito, R. V. Blanck, N. G. Harper, J. R. Hsu, and J. M. Wilken, "How does ankle-foot orthosis stiffness affect gait in patients with lower limb salvage?," *Clin. Orthop. Relat. Res.*, 2014, doi: 10.1007/s11999-014-3661-3.
- [66] Å. Bartonek, M. Eriksson, and E. M. Gutierrez-Farewik, "A new carbon fibre spring orthosis for children with plantarflexor weakness," *Gait Posture*, 2007, doi: 10.1016/j.gaitpost.2006.07.013.
- [67] S. I. Wolf, M. Alimusaj, O. Rettig, and L. Döderlein, "Dynamic assist by carbon fiber spring AFOs for patients with myelomeningocele," *Gait Posture*, 2008, doi: 10.1016/j.gaitpost.2007.11.012.
- [68] S. Yamamoto, A. Hagiwara, T. Mizobe, O. Yokoyama, and T. Yasui, "Development of an ankle-foot orthosis with an oil damper," *Prosthet. Orthot. Int.*, 2005, doi: 10.1080/03093640500199455.
- [69] Å. Bartonek, M. Eriksson, and E. M. Gutierrez-Farewik, "Effects of carbon fibre spring orthoses on gait in ambulatory children with motor disorders and plantarflexor weakness,"

- Dev. Med. Child Neurol.*, 2007, doi: 10.1111/j.1469-8749.2007.00615.x.
- [70] K. E. Gordon, G. S. Sawicki, and D. P. Ferris, "Mechanical performance of artificial pneumatic muscles to power an ankle-foot orthosis," *J. Biomech.*, 2006, doi: 10.1016/j.jbiomech.2005.05.018.
- [71] D. P. Ferris, K. E. Gordon, G. S. Sawicki, and A. Peethambaran, "An improved powered ankle-foot orthosis using proportional myoelectric control," *Gait Posture*, 2006, doi: 10.1016/j.gaitpost.2005.05.004.